BIOLOGY OF REPRODUCTION 85, 208–217 (2011)
Published online before print 6 April 2011.
DOI 10.1095/biolreprod.111.090837

Homologous Recombination in Rat Germline Stem Cells[1]

Mito Kanatsu-Shinohara,[2,6] Megumi Kato-Itoh,[3,7] Masahito Ikawa,[8] Masanori Takehashi,[4,6] Makoto Sanbo,[7] Yuka Morioka,[5,8] Takashi Tanaka,[6] Hiroko Morimoto,[6] Masumi Hirabayashi,[7] and Takashi Shinohara[6,9]

Department of Molecular Genetics,[6] Graduate School of Medicine, Kyoto University, Kyoto, Japan
Center for Genetic Analysis of Behavior,[7] National Institute for Physiological Sciences, Okazaki, Aichi, Japan
Research Institute for Microbial Diseases,[8] Osaka University, Osaka, Japan
Japan Science and Technology Agency,[9] CREST, Kyoto, Japan

ABSTRACT

Spermatogonial stem cells (SSCs) are the only stem cells in the body with germline potential, which makes them an attractive target for germline modification. We previously showed the feasibility of homologous recombination in mouse SSCs and produced knockout (KO) mice by exploiting germline stem (GS) cells, i.e., cultured spermatogonia with SSC activity. In this study, we report the successful homologous recombination in rat GS cells, which can be readily established by their ability to form germ cell colonies on culture plates whose surfaces are hydrophilic and neutrally charged and thus limit somatic cell binding. We established a drug selection protocol for GS cells under hypoxic conditions. The frequency of the homologous recombination of the *Ocln* gene was 4.2% (2 out of 48 clones). However, these GS cell lines failed to produce offspring following xenogeneic transplantation into mouse testes and microinsemination, suggesting that long-term culture and drug selection have a negative effect on GS cells. Nevertheless, our results demonstrate the feasibility of gene targeting in rat GS cells and pave the way toward the generation of KO rats.

developmental biology, gametogenesis, sertoli cells, spermatogenesis, testis

INTRODUCTION

Techniques that produce knockout (KO) animals have been established by using embryonic stem (ES) cells. The application of ES cell-based technology to a wide range of animals, however, is limited due to a lack of germline-competent ES cells in many animal species [1]. As laboratory mice do not serve as adequate models, particularly for physiology and complex disease and pharmacological studies, attempts have been made to extend KO technologies to a wider range of animal species [2]. For example, recent studies showed the advantage of using three inhibitors for glycogen synthase kinase 3 beta, mitogen-activated protein kinase kinase, and fibroblast growth factor (FGF) receptor in the derivation of germline-competent rat ES cells [3–5]. Spermatogonial stem cells (SSCs) provide the foundation of spermatogenesis throughout the life cycle of male animals. While there are only a few of these cells in the testes (0.02%–0.03% of total germ cells) [6, 7], they produce a vast amount of sperm through self-renewal and differentiation. In 1994, the spermatogonial transplantation technique was developed in which SSCs recolonize the niche and proliferate to differentiate into sperm when injected into the seminiferous tubule of testes [8]. Offspring can be produced from donor-derived SSCs [9]. Although it has been shown that SSCs rarely acquire pluripotency [10], SSCs are normally unipotent and are specialized for sperm production. However, because SSCs can proliferate indefinitely by self-renewal and can transmit genetic information to the next generation via sperm, the spermatogonial transplantation technique opened up a new avenue for germline modification.

In 2003, we established a long-term culture of mouse SSCs that were designated germline stem (GS) cells [11]. In the presence of the glial cell line-derived neurotrophic factor (GDNF), a self-renewal factor of SSCs [12], germ cell colonies of unique shape were derived from dissociated testes cells in vitro. Mouse GS cells continued to proliferate without losing their normal karyotype and genomic imprinting patterns. Moreover, GS cells possess a very stable germline potential and produce normal, fertile offspring even after 2 yr of culture [13]. In contrast, ES cells often lose germline potential during long-term culture and accumulate changes in karyotype and DNA methylation patterns [14, 15]. GS cells can be cultured under serum- and feeder-free conditions and can be genetically manipulated [16, 17]. We produced transgenic and KO mice through genetic transduction and drug selection [18]. The frequency of homologous recombination was 1.7% in mouse GS cells, which was comparable to that achieved in ES cells. Thus, SSCs have the potential to serve as an alternative to ES cells in germline modification.

The rat has been used as an animal model for medical research for over 150 yr and has advantages over mice in several areas, particularly for physiological and pharmacological studies [2]. Methods to manipulate rat SSCs have now

[1]Supported by the Genome Network Project, Japan Science and Technology Agency, CREST, Program for Promotion of Basic and Applied Researches for Innovations in Bio-oriented Industry, the Ministry of Health, Labour, and Welfare, the Cabinet Office, Government of Japan, through its Funding Program for Next Generation World-Leading Researchers, the Cooperative Study Program of the National Institute for Physiological Sciences, and the Ministry of Education, Culture, Sports, Science, and Technology.
[2]Correspondence: FAX: 81 75 751 4169;
e-mail: mshinoha@virus.kyoto-u.ac.jp
[3]Current address: Japan Science and Technology Agency, ERATO, Nakauchi Stem Cell and Organ Regeneration Project, Minato-ku, Tokyo 108-8639, Japan.
[4]Current address: Laboratory of Pathophysiology and Pharmacotherapeutics, Faculty of Pharmacy, Osaka Ohtani University, Tondabayashi, Osaka 584-8540, Japan.
[5]Current address: Institute for Genetic Medicine, Hokkaido University, Hokkaido 060-0815, Japan.

Received: 6 January 2011.
First decision: 27 January 2011.
Accepted: 17 March 2011.

eISSN: 1529-7268 http://www.biolreprod.org
ISSN: 0006-3363

been developed, and recent studies have shown that xenogeneic transplantation of rat SSCs in immunodeficient nude mice not only allowed spermatogenesis but also resulted in rat offspring production following microinsemination [19]. Transgenic rats were also produced by transducing SSCs in vitro and transplanting them into mouse or rat testes [20, 21]. Furthermore, long-term culture of rat SSCs has been established and used for generating KO rats by transposon mutagenesis [22–24]. However, unlike SSCs in vivo, rat GS cells proliferate more slowly than those of mice, and the overall efficiencies of the in vitro culture and transplantation technique are still limited. In this study, we report a simple method for deriving rat GS cells and also demonstrate homologous recombination in rat GS cells.

MATERIALS AND METHODS

Animals and GS Cell Culture

GS cells were established using two transgenic rat lines, *TgN(act-EGFP)Osb4*, Sprague-Dawley (SD) background (a gift from Dr. M. Okabe, Osaka University, Japan) or *Tg(CAG-Venus)* rats (Wistar background). The spermatogonia, spermatocytes, and round spermatids of these transgenic rats express the enhanced green fluorescent protein (EGFP) or green fluorescent protein Venus, respectively. In some experiments, *TgN(act-EGFP)Osb4* rats were mated with wild-type (wt) rats of Wistar, Donryu, Brown Norway (BN), or Lewis background to derive F1 offspring (Japan SLC, Hamamatsu, Shizuoka, Japan).

To derive GS cells, testis cells were dissociated by using a two-step enzymatic digestion using collagenase type IV and trypsin (both from Sigma, St. Louis, MO), as previously described [11]. Dissociated cells were plated on a low-cell-binding dish (Nalge Nunc International KK, Tokyo, Japan) at a density of 10^6 cells/9.6 cm^2. After being incubated for 7 to 10 days, the floating cells were removed by aspiration, and the plates were washed with fresh medium to recover adherent cells. The cells were then transferred to plates coated with laminin (20 μg/ml; BD Biosciences, Bedford, MA) at a concentration of 3×10^3 to 1×10^4 cells/cm^2. After testicular somatic cells were eliminated, the cells were maintained on laminin or mouse embryonic fibroblasts (MEFs) and were passaged every 5–7 days by incubation with Accutase (Sigma) for 10 min.

The culture medium consisted of StemPro-34 SFM (Invitrogen, Carlsbad, CA), 25 μg/ml insulin (Nacalai Tesque Inc., Kyoto, Japan), 100 μg/ml transferrin, 60 μM putrescine, 30 nM sodium selenite, 6 mg/ml D-(+)-glucose, 30 μg/ml pyruvic acid, 1 μl/ml DL-lactic acid, 2 mM L-glutamine, 5×10^{-5} M 2-mercaptoethanol, 10^{-4} M ascorbic acid, 10 μg/ml D-biotin, 30 ng/ml β-estradiol, 60 ng/ml progesterone, 3 μg/ml heparin (all from Sigma), MEM vitamin solution, MEM nonessential amino acids solution (both from Invitrogen), 20 ng/ml mouse epidermal growth factor (BD Biosciences), 10 ng/ml human FGF2, 10 ng/ml mouse FGF9, 15 ng/ml recombinant rat GDNF (all from Peprotech Inc., Rocky Hill, NJ), and 10^3 units/ml ESGRO (murine leukemia inhibitory factor; Millipore, Billerica, MA). After cells were transferred from the low-cell-binding plate, the medium was supplemented with 0.06% fetal bovine serum (Hyclone Laboratories, Inc., Logan, UT) and vitamin A-deficient B27 (Invitrogen). At approximately 1 mo after the culture was initiated, ESGRO was removed, and the serum concentration was increased to 0.2%. For culturing on MEFs, bovine serum albumin (MP Biomedicals Inc., Irvine, CA) was added at a concentration of 5 mg/ml, and the concentration levels of FGF2, FGF9, and GDNF were increased to 50, 30, and 45 ng/ml, respectively.

Flow Cytometry

The primary antibodies used were biotin-conjugated anti-rat/mouse CD90.1 (HIS51; eBioscience, San Diego, CA), purified mouse anti-rat CD9 (RPM.7), biotin-conjugated hamster anti-rat CD29 (Ha2/5; both from BD Biosciences), and mouse anti-rat GFRA1 (81401; R&D Systems, Minneapolis, MN). Allophycocyanin-conjugated goat anti-mouse immunoglobulin G (BD Biosciences), and allophycocyanin-conjugated streptavidin (eBioscience) were used to detect the primary antibodies. Stained cells were analyzed by using a FACSCalibur unit (BD Biosciences).

Transfection of GS Cells

GS cells, which were cultured for 2–5 mo (5–20 passages) after the initiation of culture, were used for transfection. For retroviral transfection, GS cells were infected with ROSAbetageo retrovirus (a gift from Dr. P. Soriano, Fred Hutchinson Cancer Center) [25]. Virus particles were produced by transient transfection of Plat-E cells with ROSAbetageo and pCMV-vesicular stomatitis virus glycoprotein plasmids as described previously [18, 26]. The titer of the virus supernatant was determined by using a Retro-X quantitative RT-PCR (qRT-PCR) titration kit (Clontech, Mountain View, CA). The infection of GS cells with the retrovirus was performed as described previously [27]. In brief, 1×10^5 GS cells were suspended in 0.8 ml of virus supernatant (0.8 ml in a 12-well plate) in the presence of 10 μg/ml polybrene (Sigma) and plated on MEFs. The plate was then centrifuged at $3000 \times g$ for 1 h at 32°C. The plate was incubated overnight, and the cells were passaged on the next day after infection. The final titer of the retrovirus concentrate was adjusted to 2.9×10^6 colony-forming units (cfu) per milliliter. In experiments carried out under normoxic conditions, GS cells were transduced at 9.1×10^7 cfu/ml.

Plasmid DNAs were electroporated into GS cells using cell line Nucleofector kit T (Lonza, Münster, Germany) according to the manufacturer's instructions. Briefly, 4×10^6 GS cells were suspended in 100 μl of Nucleofector solution T mixed with 5 μg of DNA and subjected to electroporation using program A-23. For homologous recombination, a gene targeting vector was constructed with the use of pNT1.1 containing the *Neo* and thymidine kinase genes [28]. A 2.8-kb *Not*I-*Xho*I fragment and a 6.5-kb *Kpn*I-*Xba*I fragment of the *Ocln* gene were inserted as short and long arms, respectively. In some experiments, the vector was linearized by *Not*I digestion.

After electroporation, cells were split into 3 wells of a 12-well culture plate that had been plated with G418-resistant MEFs. Genetic selection was carried out with 40 μg/ml G418 (Invitrogen) [17]. After incubation with G418 for approximately 2–3 wk, the contents of each well were passaged at a 1:1 ratio in a well of a fresh 12-well culture plate. As the growth of GS cells was density dependent [17], 1×10^5 nontransfected wt GS cells were added two to three times to each well at passage. It generally took 3–4 mo to establish G418-resistant clones. A negative selection marker (*tk*) was not used in these experiments. To enhance the efficiency of genetic selection, the cells were cultured in 5% O_2 in some experiments. Colonies resistant to G418 were screened by PCR, using the specific primers listed in Supplemental Table S1 (available online at www.biolreprod.org). The selected cells were cryopreserved in a cryopreservation solution (Cellbanker; Dia-Iatron, Tokyo, Japan), using previously described procedures [29].

Southern Blot Analyses

Positive clones were confirmed by Southern blot analysis using *Eco*RV digestion and hybridization with a 344-bp probe derived from intron 1, which was produced by PCR amplification using the specific primers listed in Supplemental Table S1.

Transplantation Procedure

GS cells were microinjected into the seminiferous tubules of KSN nude mice (Japan SLC, Inc., Shizuoka, Japan) that were treated with 44 mg/kg busulfan at 4 wk of age. Busulfan-treated mice received transplants of syngeneic bone marrow cells 2–4 days after treatment to avoid bone marrow suppression. These animals were used for germ cell transplantation at least 4 wk after busulfan treatment. A single-cell suspension containing approximately 4×10^4 to 8×10^4 cells (for counting colonies) or 10^6 cells (for microinsemination) was introduced into the seminiferous tubules via the efferent duct. Each injection filled 75%–85% of the total tubules. The Institutional Animal Care and Use Committee of Kyoto University approved all of the animal experimentation protocols.

Analysis of the Recipient Testes

To quantify germ cell colonies, we recovered recipient testes 3 mo after transplantation and exposed them to ultraviolet (UV) light. The donor cell-derived fluorescence was observed under a stereomicroscope. The donor cell clusters were defined as colonies when they occupied the entire basal surface of the tubule and were at least 0.1 mm in length.

For histological analysis of the testes, testis samples were collected and fixed in 2% paraformaldehyde. The sample was then embedded in Tissue-Tek OCT compound (Sakura Finetechnical, Tokyo, Japan) for cryosectioning. Meiosis was detected by immunofluorescence, using rabbit antisynaptonemal complex protein 3 (SYCP3) antibodies, which were prepared by using a synthetic oligopeptide (a gift from Dr. S. Chuma, Kyoto University, Japan) [30]. Alexa 568-conjugated goat anti-rabbit immunoglobulin was used as a secondary antibody (Invitrogen). Sections were counterstained with Hoechst 33342 dye (Sigma). Images of the sections were obtained using a confocal microscope (Fluoview FV1000D; Olympus, Tokyo, Japan).

Combined Bisulfite Restriction Analysis (COBRA)

Genomic DNA was treated with sodium bisulfite, which deaminates unmethylated cytosines to uracils but does not affect 5-methylated cytosines. With this template, differentially methylated regions (DMRs) of the indicated genes were amplified by PCR with the specific primers listed in Supplemental Table S1. The PCR products were digested with the indicated restriction enzymes, which recognize sequences containing cytosine-phosphate-guanine in the original unconverted DNA. The intensity of the digested bands was quantified using Image Gauge software (Fuji Photo Film, Tokyo, Japan).

Microinsemination

Spermatogenic cells were collected from the recipient testes by repeated pipetting of the seminiferous tubule segments that showed EGFP or Venus fluorescence. Microinsemination was performed as described previously, using round spermatids [19]. The constructed embryos were cultured for 24 h and transferred into the oviducts of pseudopregnant Wistar rats. Offspring were recovered by cesarean section at 21 days after transfer.

Karyotype Analysis

Cultured cells were harvested, treated with 75 mM KCl for 15 min, and fixed with a methanol-acetic acid (3:1) solution. Metaphase spreads were prepared using standard procedures, and the slides were stained with Hoechst 33258 dye (Sigma).

Statistical Analysis

The results are presented as means ± SEM. Data were analyzed using a Student *t*-test for independent samples with equal variance.

RESULTS

Derivation of Rat GS Cells by Selection with a Low-Cell-Binding Plate

To establish rat GS cells, testis cells from 12- to 18-day-old *TgN(act-EGFP)Osb4* rats were dissociated with enzymatic digestion. Given that the culture medium for mouse GS cells induces overgrowth of somatic cells and inhibits germ cell growth, we modified the culture medium by reducing the serum concentration and supplementing it with FGF9, which has beneficial effects on primordial germ cells and spermatogonia [31, 32]. We also employed a low-cell-binding plate to reduce the attachment of somatic cells. Under these conditions, spermatogonia preferentially attached to the plate, whereas most somatic cells floated in the medium (Fig. 1A). After 6–8 days of culture, spermatogonia clumps were dissociated with gentle pipetting and transferred to a laminin-coated culture plate. The cells then started to form chain-type colonies (Fig. 1B) and could be easily distinguished from somatic cells, which showed a larger, fibroblast-like appearance. In contrast, germ cells plated after gelatin selection could not produce colonies due to somatic cell overgrowth (Fig. 1C). Whereas somatic cells stopped proliferating during repeated passages, germ cells continued to proliferate on laminin-coated plates. Approximately 1 mo after culture was initiated, these colonies consisted entirely of germ cells (Fig. 1D, left). Flow cytometric analysis confirmed that the cultured cells expressed several SSC markers, including ITGB1, CD9, and THY1 (formerly CD90) (Fig. 1E). The cells also expressed GFRA1, but its expression level was variable, indicating that they are a heterogeneous population. Established GS cells proliferated constantly for a long term, and the total cell number increased 2.6×10^{55}-fold over 822 days (between 100 and 922 days) (Fig. 1F).

Stem cell activities of cultured cells were assessed by spermatogonial transplantation. Because rat SSCs reinitiate spermatogenesis and produce offspring following transplantation into xenogeneic mouse testes [19], we used immunodeficient nude mice as recipients. Two independent cultures were maintained and injected into the seminiferous tubules of busulfan-treated nude mice. Three months after transplantation, the testes were examined for the presence of EGFP-expressing germ cell colonies under UV fluorescence. While culture 1 showed 2.2×10^{55}-fold increase in the number of SSC cells over 822 days of culture (between 100 and 922 days), SSCs in culture 2 showed 6.1×10^{11}-fold expansion after 222 days (between 116 and 338 days; Table 1). Colonization efficiencies did not change significantly during the experimental period. The cells maintained in vitro for 116 or 443 days produced offspring resulting from microinsemination using round spermatids in the recipient testes.

Genetic Selection of Rat GS Cells

Next, we examined conditions for genetic selection. GS cells established from *TgN(act-EGFP)Osb4* or *Tg(CAG-Venus)* rats were transduced with the retrovirus vector ROSAbetageo, which expresses beta-galactosidase and becomes G418-resistant under the promoter of trapped genes [25]. Transduced cells were cultured on laminin, and G418 was added to the culture at 10 days after infection. Although LacZ staining confirmed the transduction of GS cells, we could not establish GS cell transfectants with G418 selection under those culture conditions.

Then we selected G418-resistant cells using the MEF feeder. Although GS cells form flat chain- or monolayer-type colonies on laminin, they form three-dimensional clump-type colonies on the MEF feeder (Fig. 1D, right). However, proliferation of rat GS cells was less efficient on MEFs than on laminin (Fig. 1G). Under the MEF-based culture, we obtained a few G418-resistant colonies. Given that the

TABLE 1. SSC expansion in long-term culture.

Culture	Days to transplant[a] (passage)	Colonies/10^5 GS cells (no. of recipient testis)[b]	Increase in total cell no. (fold)[c]	Increase in SSC no. (fold)[d]
1	100 (8)	251.4 ± 13.1 (4)	-	-
	172 (16)	70.6 ± 15.7 (4)	1.7×10^3	466.2
	351 (37)	493.3 ± 149.6 (6)	3.4×10^{13}	6.7×10^{13}
	443 (48)[e]	310.0 ± 63.4 (6)	5.2×10^{18}	6.4×10^{18}
	922 (114)	210.0 ± 58.6 (3)	2.6×10^{55}	2.2×10^{55}
2	116 (10)[e]	137.3 ± 20.3 (4)	-	-
	338 (35)	332.5 ± 33.8 (8)	2.5×10^{11}	6.1×10^{11}

[a] The number of days from initiation of culture to transplantation.
[b] Values are means ± SEM.
[c,d] The increase in the total cell or SSC number from the initial transplantation indicated.
[e] These cultures produced offspring by microinsemination.

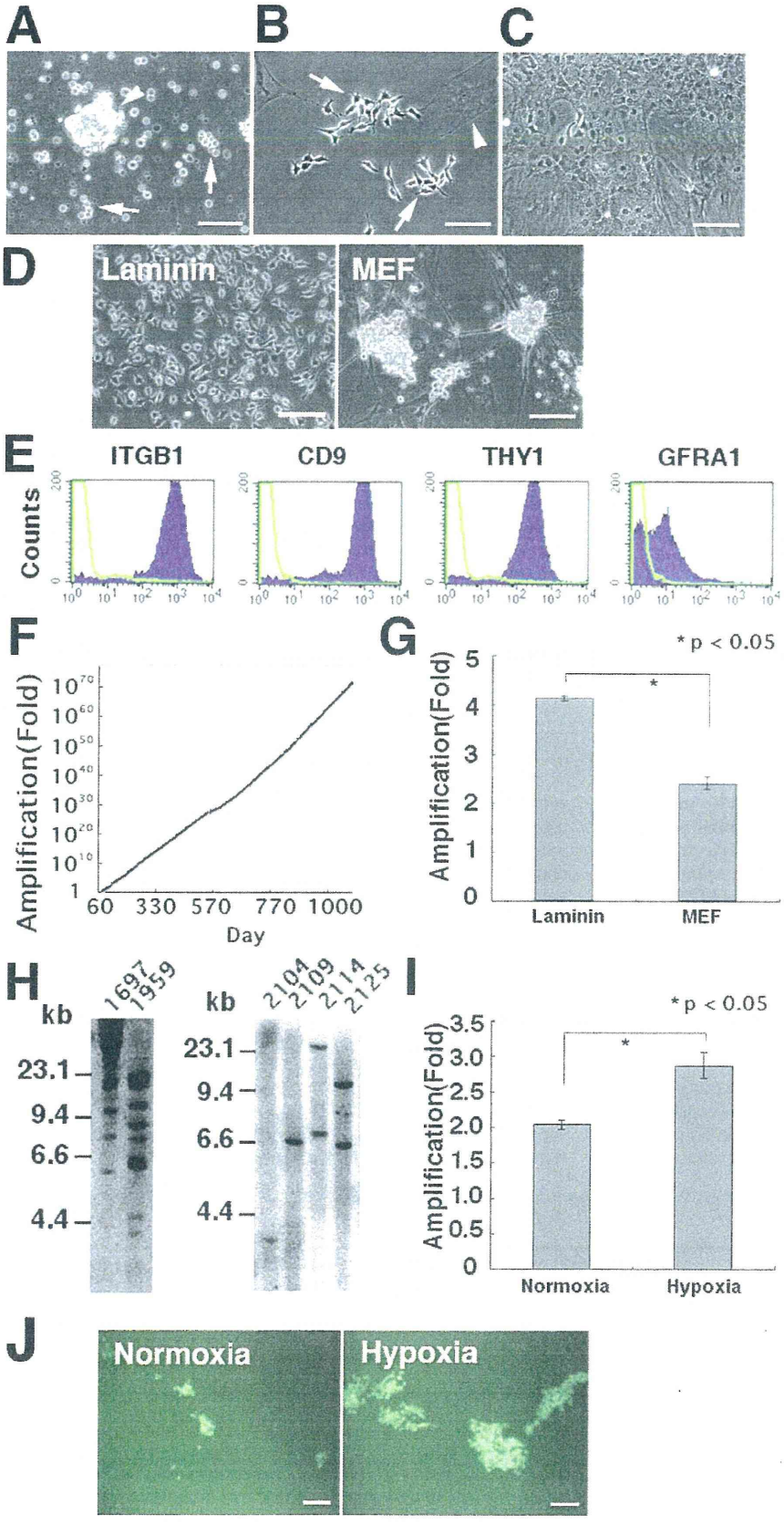

FIG. 1. Long-term culture and drug selection of rat GS cells. **A**) Germ cell colonies that developed on a low-cell-binding plate 7 days after culture initiation are shown. While germ cells were loosely attached to the plate and proliferated (arrows), somatic cells aggregated to form floating clumps (arrowhead). **B**) Proliferation of germ cells is shown 4 days after transfer to a laminin-coated plate. While few somatic cells (arrowhead) remained in culture, germ cells were relatively enriched (arrows). **C**) Rat testis cells cultured on tissue culture dish are shown 6 days after gelatin selection. Germ cell proliferation was suppressed by the overgrowth of testicular somatic cells. **D**) Established rat GS cells cultured on a laminin-coated plate (left) and MEFs (right) are shown. **E**) Flow cytometry of GS cells was performed. Green lines indicate control staining. **F**) Growth curve of GS cells on laminin is shown. **G**) Proliferation of GS cells grown on laminin and MEFs are shown during 5 days of culture ($n = 4$). The difference was significant. **H**) Southern blot analyses of G418-resistant GS cell clones are shown. A full-length *Neo* fragment was used as a probe. Genomic DNA was digested with *Eco*RI, which does not cut the retrovirus vector. Clones with multiple integrations were observed when the cells were selected under normoxic conditions (left), whereas selection under hypoxic conditions allowed clones to establish a single/low number of integrations (right). **I**) Enhanced proliferation of rat GS cells on hypoxic MEFs ($n = 3$) is shown. GS cells, which had been cultured for 3 mo from the time of culture initiation, were plated at 3×10^5 cells/9.4 cm^2. Increase in GS cell numbers after 5 days of culture is shown. **J**) Large colony formation after 11 days of G418 selection on hypoxic MEFs (right) is shown. Identical GFP-expressing *Neo*-resistant GS cells (8000 cells), which had been cultured for 7 mo, were mixed with 4×10^4 cells/9.4 cm^2 on MEFs and incubated in the presence of G418 under normoxic and hypoxic conditions, respectively. Significantly smaller colonies were formed under normoxic conditions (left). Bar = 100 μm (**A–D**) and 50 μm (**J**).

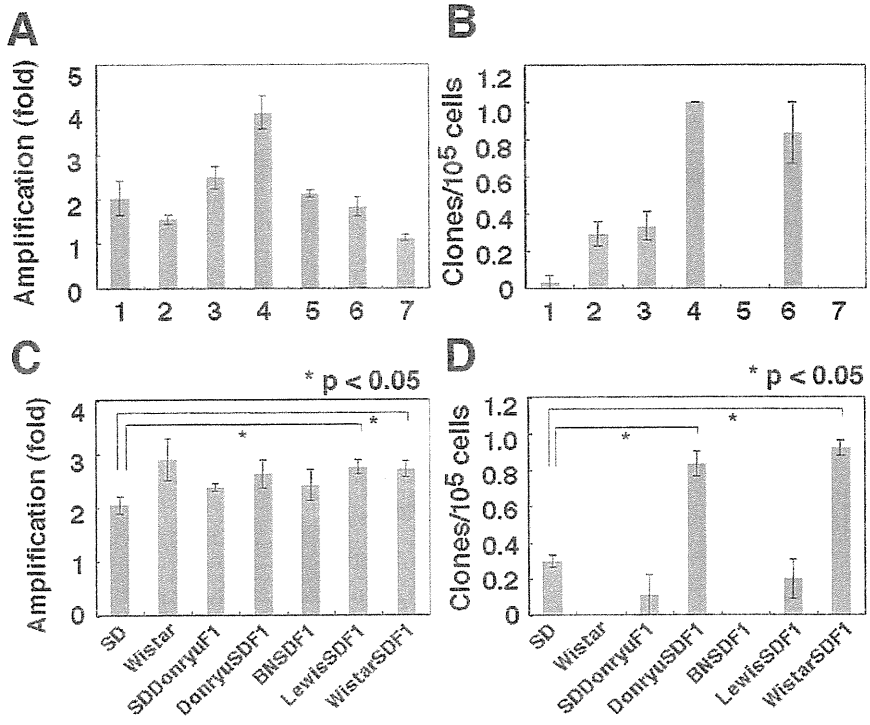

FIG. 2. Variations in the efficiencies of drug selection among GS cell clones are shown. **A**, **B**) Efficiencies of proliferation (**A**) and clone establishment (**B**) are shown using seven GS cell lines (1–7) in an SD background. To evaluate proliferation, GS cells were harvested at 2.8×10^5 cells/9.6 cm^2 on a laminin-coated dish, and the number of cells after 6 days of culture was counted (n = 4). To evaluate drug selection efficiency, GS cells were infected with ROSAbetageo virus, and the number of clones established by infecting 1×10^5 cells/3.8 cm^2 GS cells after selection with G418 in at least six experiments is shown. **C**, **D**) Efficiencies of proliferation (**C**) and clone establishment (**D**) are shown using GS cell lines of variable genetic backgrounds. To evaluate proliferation, GS cells were harvested at 2.8×10^5 cells/9.6 cm^2 on a laminin-coated dish, and the number of cells after 6 days of culture were counted. Three independent GS cell lines of each strain were examined (n = 10). Asterisks indicate strains that are significantly different from SD ($P < 0.05$). To determine drug selection efficiency, the number of clones established by infecting 1×10^5 cells/3.8 cm^2 GS cells after selection with G418 in at least nine experiments is shown. At least two lines were used in each experiment.

efficiency of G418-resistant colony development was significantly lower, we then used a virus supernatant, which was concentrated by centrifugation, and established 45 clones from $\sim 1.6 \times 10^7$ cells in 13 experiments. However, Southern blot analysis using a *Neo* probe showed multiple transgene integrations in all clones (Fig. 1H, left). This result suggested that only clones expressing the G418-resistant gene at high levels were selected by this method.

Because limited proliferation of GS cells on MEFs reduced drug selection efficiency, we tried to improve the GS cell culture conditions by reducing oxygen levels [22]. The proliferation of rat GS cells was 1.4-fold enhanced within 5 days of culturing on hypoxic MEFs (Fig. 1I). Hypoxia also improved drug selection efficiency. While the G418-resistant cells formed colonies of moderate size after 11 days of selection under normoxia (Fig. 1J, left), we observed significantly larger colonies under hypoxia during the same period (Fig. 1J, right). In contrast, hypoxia did not influence viability of GS cells; viability levels of wt GS cells after 11 days of selection, as assessed by trypan blue exclusion, were 23.7% ± 0.9% (n = 6) and 28.6% ± 3.2% (n = 6) for normoxia and hypoxia, respectively, and the difference was not significant. Under this condition, 50 clones with ~1–2 integrations were reproducibly established from $\sim 4.2 \times 10^7$ GS cells in 70 experiments by transducing 30 independent GS cell lines (Fig. 1H, right).

We then examined the efficiencies of growth and drug selection by using several GS cell lines (Fig. 2, A and B). Although seven GS clones in an SD background appeared morphologically indistinguishable, no clones were established from the two lines. The growth rate of seven GS cell lines also varied, but the growth rate did not correlate necessarily with the genetic selection efficiency. To examine whether the selection efficiency was influenced by the genetic background of GS cells, we established GS cell lines from various strains and compared the efficiencies of growth and genetic selection (Fig. 2, C and D). Although these cells proliferated at a comparable speed, we observed significant variations in selection efficiencies. While GS cells of SD background produced ~0.3 clones/10^5 cells, no clones were established from GS cells from a Wistar background. GS cells from both DonryuSDF1 and WistarSDF1 hybrids exhibited significantly higher efficiency,

TABLE 2. Offspring production from ROSAbetageo-infected GS cells by microinsemination.

Source of round spermatid	Host oocyte strain	No. of oocytes (%)			No. (%)	
		Injected	Survived	Transferred	Implantations	Pups born
ROSAbetageo-infected GS cells						
886 (SD)	SD	1482	1184 (80)	1089	75 (7)	18 (2)
1122 (Wistar)	SD	154	115 (75)	100	61 (61)	33 (33)
1176 (Wistar)	SD	587	401 (68)	334	154 (46)	64 (19)
Total		2223	1700 (76)	1523	290 (19)	115 (8)
Control						
Nonmanipulated GS cells (SD)	SD	144	94 (65)	74	20 (27)	4 (5)
Fresh round spermatid (SD)	SD	150	130 (87)	129	49 (38)	21 (16)
Fresh round spermatid (Wistar)	SD	306	220 (72)	205	83 (40)	34 (17)

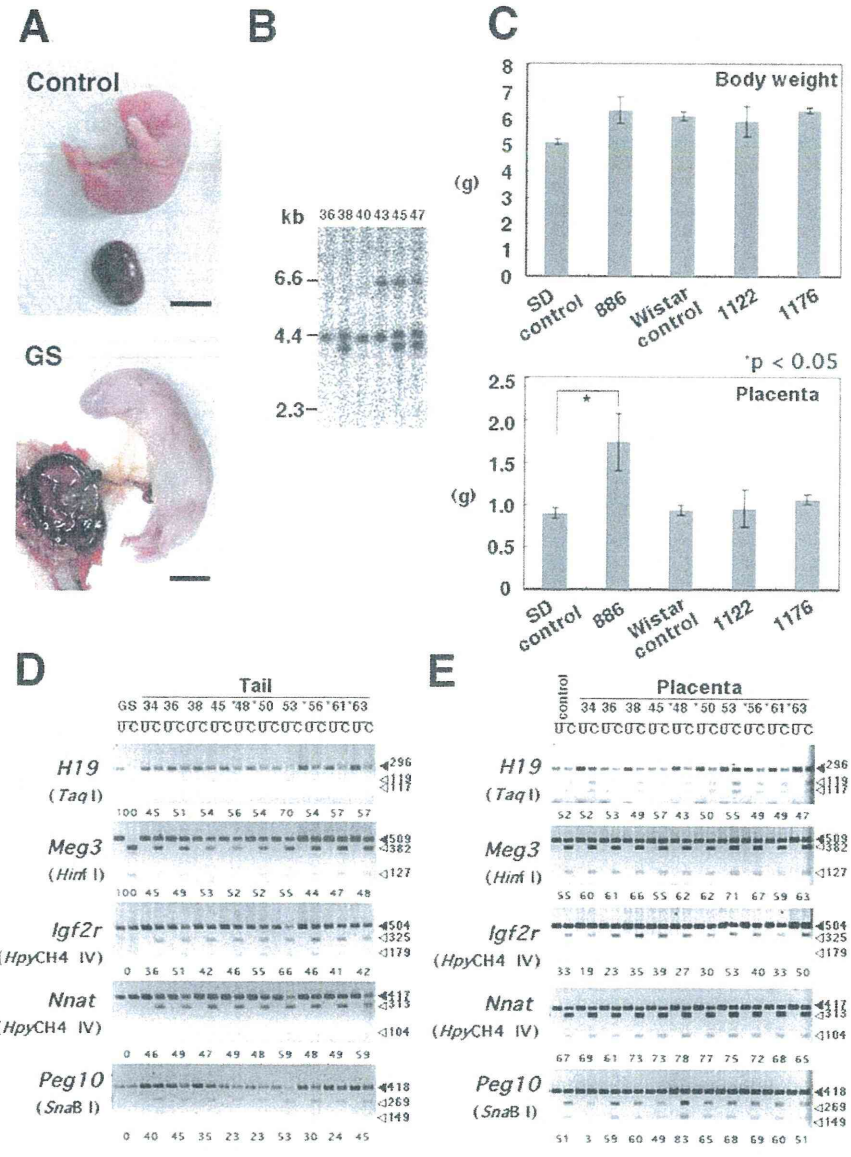

FIG. 3. Offspring produced from GS cell clones are shown. **A**) Offspring derived from the wt (SD) (top) or GS cell (clone 886)-derived round spermatids (bottom) by microinsemination are shown. Note the enlarged placenta of the offspring derived from GS cells. **B**) Southern blot analysis of offspring DNAs derived from GS cell (clone 886)-derived round spermatids is shown. Genomic DNAs from six offspring were digested with *Eco*RI, which does not cut the retrovirus vector. A full-length *Neo* fragment was used as a probe. **C**) Weights of offspring (top) and placenta (bottom) are shown. Offspring from GS cells (886) had significantly enlarged placentas (n = 12 for clone 886 and clone 1122; n = 21 for the control SD round spermatid; n = 33 for the control Wistar round spermatid, and n = 34 for clone 1176). **D**, **E**) COBRA of the tail (**D**) and placenta (**E**) DNA in 10 different offspring. Asterisks indicate placentas that weighed >2.0 g. Open and closed arrowheads indicate the size of methylated and unmethylated DNA, respectively. Placenta derived from microinsemination using wt sperm of SD rat was used as a control. The enzymes used to cleave each locus are indicated in parentheses. U, uncut; C, cut. Bar = 1 cm (**A**).

but those from other F1 hybrids (SDDonryuF1, BNSDF1, and LewisSDF1) showed limited efficiency. These results suggest that growth speed is not correlated with the genetic selection efficiency.

Offspring Production from Genetically Selected Rat GS Cells

To investigate whether genetically manipulated GS cells maintain the potential to produce normal offspring after drug selection, we injected several clones into seminiferous tubules of busulfan-treated nude mice. At 3–6 mo after transplantation, EGFP-expressing colonies were dissected and used for microinsemination. Round spermatids from clones 886, 1122, and 1176 were recovered from the recipient testes and microinjected into SD oocytes. In total, 2223 oocytes were injected, and 115 offspring were recovered by cesarean section (Fig. 3A; Table 2). Southern blot analysis with *Neo* probe confirmed germline transmission of transgene (Fig. 3B).

Although the offspring produced from the GS cells appeared normal, we noted large placentas for several of them. While clones 1122 and 1176 exhibited a normal range of placenta weight (0.95 ± 0.22 g, n = 12 for clone 1122; 1.02 ± 0.06 g, n = 34 for clone 1176), the average weight of the placentas derived from clone 886 was 1.74 ± 0.33 g (n = 12), which was significantly heavier than the control, using fresh wt round spermatids (0.93 ± 0.06 g, n = 33 for Wistar; 0.90 ± 0.06 g, n = 21 for SD) (Fig. 3, A and C; and see Supplemental Table S2). We also examined the DNA methylation patterns in DMRs of several imprinted genes. Genomic DNAs from GS cells, tails, and placentas of the offspring derived from clone 886 were analyzed by using COBRA. Methylation at the loci of the paternally imprinted *H19* and *Meg3* genes and maternally imprinted *Igf2r*, *Nnat* (formerly *Peg5*), and *Peg10* genes was analyzed. GS cells showed typical androgenetic imprinting patterns, with hypermethylation in the *H19* and *Meg3* DMRs and hypomethylation in the *Igf2r*, *Nnat*, and *Peg10* genes, whereas DMR methylation in the tail DNA showed somatic

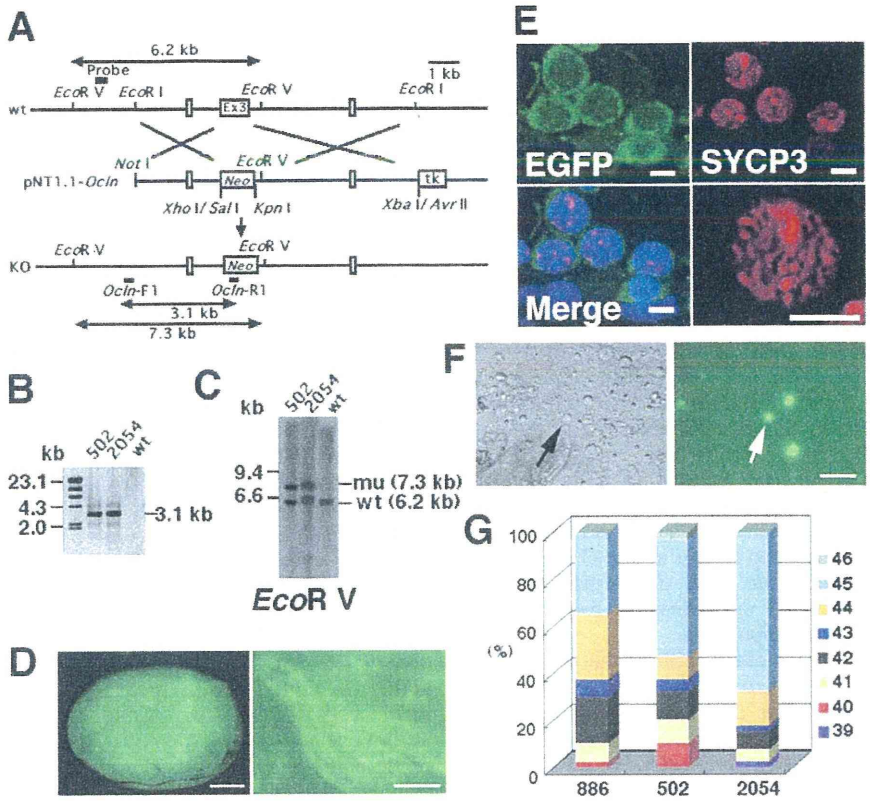

FIG. 4. Homologous recombination in GS cells is shown. **A**) Targeting vector of the *Ocln* gene. Exon 3 (Ex3) was replaced with the *Neo* gene. PCR primers and a probe for Southern blotting are shown. **B**, **C**) PCR (**B**) and Southern blot (**C**) analyses of two clones demonstrating homologous recombination are shown. Genomic DNAs of GS cell clones were digested with *Eco*RV. **D**) Colonization of a GS cell clone (2054) in seminiferous tubules of nude mice 3 mo after transplantation. Low (left) and high (right) magnification. **E**) Histological appearance of a recipient mouse testis stained with anti-SYCP3 antibodies. The donor-derived germ cells (green) displayed the formation of synaptonemal complexes with SYCP3 fluorescence (red), indicating meiosis of the donor rat cells in the mouse testis. The section was counterstained with Hoechst 33342 dye (blue). **F**) A round spermatid derived from donor SSCs is shown. Green fluorescence indicates the donor cell origin. **G**) Karyotype analysis is shown. Chromosome numbers of clone 886, 502, and 2054 are shown. mu, mutant. Bar = 1 mm (**D**, left), 200 μm (**D**, right), 5 μm (**E**), and 50 μm (**F**).

cell imprinting patterns. Although we noted hypermethylation of the *Peg10* gene in the placenta in one of the offspring, we did not find apparent abnormalities in other offspring with large placentas (Fig. 3, D and E). The large-placenta phenotype did not persist in the germline because two of the clone 886-derived male offspring produced normal F2 healthy offspring by microinsemination, and the sizes of their placentas were normal.

Homologous Recombination Using Rat GS Cells

Finally, to examine whether gene targeting technology is applicable to rat GS cells, we constructed a gene targeting vector for *Ocln*. GS cells established from *TgN(act-EGFP)Osb4* rats were electroporated with the targeting vector (Fig. 4A) and treated with G418 on a MEF feeder at 7–10 days after electroporation. Immediately after electroporation, 51.4% ± 3.6% (n = 3) of the input cells were recovered, and 86.9% ± 1.8% (n = 3) of them were viable. In total, by transducing 20 independent GS cell lines, 33 clones were established from ~6.4×10^8 GS cells with circular DNAs in 159 experiments; whereas 15 clones were established from ~5.8×10^8 GS cells with linearized DNAs in 144 experiments. Genomic DNAs were isolated from cultured cells and screened for clones of homologous recombination by PCR. Homologous recombination occurred in two clones transduced with circular DNAs (Fig. 4B), which was confirmed by Southern blotting (Fig. 4C). These two clones were established from two independent GS cell lines. To produce offspring, these cells were transplanted into busulfan-treated nude mice. Three months after transplantation, EGFP-expressing donor-derived colonies were detected in the recipient testes under UV light (Fig. 4D). Immunohistological examination showed that EGFP-expressing donor-derived germ cells underwent meiosis in the mouse testes, as indicated by the formation of synaptonemal complexes, which were detected by SYCP3 expression (Fig. 4E).

We collected EGFP-expressing round spermatids and performed microinsemination (Fig. 4F). A total of 1568 eggs were constructed and transferred into the uteri of pseudopregnant mothers. Although 43 embryos were implanted in the uteri, no offspring were produced from these animals (Table 3). To investigate whether genetically selected cells have normal

TABLE 3. Offspring production from gene-targeted GS cells by microinsemination.

Clone	Host oocyte strain	No. of oocytes (%)			No. (%)	
		Injected	Survived	Transferred	Implantations	Pups born
502	SD	900	688 (76)	572	22 (4)	0 (0)
2054	SD	276	211 (76)	210	6 (3)	0 (0)
2054	Wistar	221	170 (77)	162	9 (6)	0 (0)
2054	Wistar Hannover	171	138 (81)	137	6 (4)	0 (0)
Total		1568	1207 (77)	1081	43 (4)	0 (0)

karyotypes, cytogenetic analysis was conducted by using Hoechst 33258 staining. The results showed that clones 886, 502, and 2054 maintained normal karyotype (42 chromosomes) in 20.0%, 12.5%, and 7.5 % of the cells, respectively (Fig. 4G).

DISCUSSION

In this study, we demonstrated the feasibility of homologous recombination in rat GS cells. Since this technique was first reported in 1985 [33, 34], it is the most reliable method for introducing site-directed mutations in the genome of the ES cell. The efficiency of homologous recombination varies widely among different cell types and depends on multiple factors, such as the length of homology or method of transfection. For example, the reported frequency of homologous recombination can be very high in ES cells (up to 10^{-1}) but was significantly low in fertilized eggs (1/500 eggs) [35–37]. These results raise the question as to whether this technique can be used in SSCs, another potential target of germline modification. We demonstrate that the efficiency of homologous recombination in rat GS cells was 4.2%, which is comparable to that in mouse GS cells (1.7%) and in ES cells. Therefore, our study demonstrates that a reasonable level of homologous recombination occurs in rat GS cells for their genetic manipulation.

As with other species, the most difficult part of GS cell derivation is removing testicular somatic cells. In mice, gelatin-coated plates are usually used to remove somatic cells for culture initiation [11]. As somatic cells attach firmly to gelatin-coated plates, germ cells can be enriched by gentle pipetting. However, a similar approach was not applicable to enrichment of rat germ cells because rat somatic cells proliferate more actively than mouse cells, which interfered with initial germ cell colony development. This problem was resolved by cell sorting or gentle pipetting in previous studies [22, 23]. In this study, we devised the novel method of exploiting serum-free medium and a low-cell-binding plate. Under these conditions, somatic cell proliferation is effectively suppressed during culture initiation. Unexpectedly, germ cells attached loosely to the plate and could be efficiently enriched by removing floating cells. Although cell sorting may be a useful approach for the enrichment of germ cells [23], it requires time-consuming asceptic cell separation and subsequent expansion of sorted cells. In contrast, the use of a low-cell-binding plate is relatively cost effective and does not harm the cells as much as cell sorting. The attachment of spermatogonia to a low-cell-binding plate is counterintuitive but probably does not involve integrins, because cells can be easily dislodged by gentle pipetting and cell recovery does not require trypsin digestion. The cells still proliferate slowly on the plate and form clusters within several days. This technique has worked well to establish rat GS cell lines from different genetic backgrounds in our laboratory.

Serum greatly influenced the growth of rat GS cells. Although mouse GS cells proliferate efficiently and maintain SSC activity in the presence of 1% serum [11], this concentration of serum was detrimental for rat GS cells and was reduced to ~0.2%. Perhaps some factors in the serum induce stem cell differentiation, whereas other unknown components are necessary to maintain proliferation. Despite the difference in serum concentration, rat GS cells depend critically on GDNF and FGF2 for continuous proliferation, as with mouse GS cells, and show similar morphology. While the doubling time of mouse GS cells was 5.7 days on the laminin-coated dish [16], that of the rat GS cells was 2.5 days in our study. Previous transplantation studies showed that rat germ cell colonies expand significantly faster than those of mouse in the mouse seminiferous tubule [38]. The higher growth rate of rat GS cells on laminin-coated dishes is consistent with the in vivo observation and suggests that current culture conditions using laminin-coated dishes promote efficient growth.

Although rat GS cells proliferate stably on laminin-coated plates, they do not proliferate well on MEFs (doubling time, 3.9 days in normoxia). This is in contrast to mouse GS cells, which proliferate efficiently on MEFs (doubling time, 2.7 days) [11]. Unfortunately, although culturing on laminin was the most effective way to expand rat GS cells, we were not able to perform drug selection of two-dimensional colonies on laminin-coated plates. Drug selection was possible only with three-dimensional cluster-type colonies on MEFs. Selection under hypoxic conditions enhanced the efficiency of establishing G418-resistant clones. Hypoxia is reported to enhance survival and/or self-renewal of hematopoietic stem cells by stabilizing hypoxia-inducible factor 1 alpha [39, 40]. In another study, hypoxia prevented differentiation of human ES cells, possibly by modifying the growth factor expression pattern [41]. The mechanism of enhancement in genetic selection efficiency of GS cells in current study is unclear but may be caused by similar mechanisms. Although culture under hypoxic conditions achieved a doubling time of 3.3 days, rat GS cells still proliferated more slowly than mouse GS cells, and the colony morphology was less stable on MEFs. To resolve these problems, we tried cocultures with other feeder cells such as rat embryonic fibroblasts, STO, Sertoli cell line 15P1, and others, but we found that MEFs gave the best results in rat GS cell maintenance (our unpublished observation). Further studies are necessary to search for better selection conditions by employing other extracellular matrix or mechanical supports, which may produce three-dimensional cluster-type colonies without growth suppression.

Given that we detected a correlation between mouse strains and GS cell growth efficiency [11], we examined the influence of genetic backgrounds on rat GS cell derivation and drug selection. In mice, the genetic background significantly influenced the efficiency of GS cell derivation and maintenance. Although DBA/2 and ICR are efficient, establishing GS cells from C57BL/6 and 129 mice is difficult or impossible [11]. In contrast, the derivation of rat GS cells was not significantly influenced by the genetic background. GS cells were easily derived from all of the tested backgrounds, and we observed no significant differences in their growth rates or colony morphologies. Despite such similarity, the drug selection efficiency was significantly different among strains. The efficiency levels at which *Neo*-resistant clones were established in Wistar, BNSDF1, SDDonryuF1, and LewisSDF1 GS cells were low, but we were able to carry out genetic selection more efficiently using GS cells from DonryuSDF1 and WistarSDF1 rats. In mice, inbred strains are known to have more variable biological responses than F1 hybrids [42]. Our results suggest that genetic factors play more important roles in rat GS cells in their response to drug selection.

The most important observation in this study was the decreased germline potential of rat GS cells. While mouse GS cells could produce offspring after 2 yr of consecutive culturing or after genetic selection [13, 17], only some of the rat GS cell clones were able to undergo germline transmission. Although we obtained offspring from ROSAbetageo virus-infected cells, we were not able to do so from the two clones that underwent homologous recombination. A similar observation was also reported in a recent study using transposon-mediated mutagenesis [24]. In that study, the problem was resolved by taking advantage of *Dazl* knockdown transgenic rats with decreased

spermatogenic potential [43]. Transplanted SSCs were able to compete well with endogenous SSCs, and the recipient rats sired donor-derived offspring. In the current study, we used xenogenic transplantation to produce offspring, due to the instability of rat testes as recipients [44]; it was reported that a return of endogenous spermatogenesis is essential for reestablishing fertility after transplantation into rat recipients. We have not experienced significant problems with xenogenic transplantation with other donor cell types, but it is possible that germline potential was compromised in mouse testes and that two-targeted clones produce functional sperm if transplanted into *Dazl* knockdown transgenic rats.

Although it was speculated that the failure to undergo germline transmission might have been caused by the disruption of spermatogenic genes [24], disruption of *Ocln* is unlikely to have influenced germline potential. Although homozygous *Ocln* KO mice are infertile, heterozygous males are fertile, and no defects in spermatogenesis were found [45]; or rather, our results suggest that abnormal karyotype of the cultured cells is responsible for reduced fertility of the genetically selected cells. We currently do not know the factors directly involved in genetic stability, but we speculate that the low serum concentration might have caused abnormal karyotype. We recently found that mouse GS cells also exhibit reduced germline potential when they are cultured under serum- and feeder-free conditions [46]. The absence of serum not only decreased colony-forming efficiency after transplantation but also reduced the success rate of microinsemination. Although rat GS cells are similar to mouse GS cells in that they require serum, rat cells are more sensitive to serum, which is probably too low to maintain normal karyotype. Considering that a similar observation was also reported for human ES cells [47], it is possible that serum contains some unidentified factor that maintains chromosomal stability. We are currently improving the rat GS cell culture conditions by modifying the medium composition. In addition, as there are variations among GS cell lines, our results suggest that selection of robust GS cell lines would be necessary for successful germline transmission.

Although some GS cells underwent germline transmission, we also found placentomegaly in the offspring. A similarly large placenta is often associated with nuclear cloning [48]. However, the exact mechanism remains unknown. The abnormal placenta development in our study was likely caused by the in vitro long-term culture because we have not encountered a similar phenomenon when we carried out microinsemination using fresh round spermatids or spermatozoa, including those that were generated in the xenogeneic seminiferous tubules [19, 20]. Although one of the offspring showed hypomethylation in the *Peg10* gene (Fig. 3D), no abnormal methylation was found in other offspring. Nevertheless, abnormal methylation in the *Peg10* gene suggests that this placental abnormality was caused by the disruption of other imprinting-related genes, and long-term culture and genetic selection of GS cells might also have induced epigenetic errors. These results suggest that rat GS cells are more vulnerable to stress during in vitro culture than mouse GS cells.

Currently, whether the problems associated with rat GS cells also apply to SSCs from other animal species is unknown. Although SSCs from different animals are being cultured [49–51], no attempts at genetic manipulation have been reported. Considering that rat SSCs can proliferate faster than mouse SSCs in vivo in mouse seminiferous tubules after xenogeneic transplantation and that transgenic rats could be produced at a relatively high efficiency after short-term culture of SSCs [20, 43], one of the obstacles may be due to the suboptimal culture conditions. Future studies must be directed to improve current SSC culture conditions by identifying factors that further facilitate SSC self-renewal.

In vitro expansion of SSCs and their transgenesis is a new approach in germline modification. The successful homologous recombination of rat GS cells provides an important step in extending this technique to rats. However, our study also revealed important problems associated with the genetic manipulation of GS cells that must be overcome to improve this technology. Despite these drawbacks, GS cells have the unique advantage of being able to contribute to the germline without chimera formation, which is a critical step in ES cell technology. Unlike ES cells, the phenotypes of GS cells are relatively stable [13–15]. Such advantages will allow a different approach. These unique features of SSCs make them an attractive alternative target for germline modification, with the final goal of genetically modifying SSCs from many animal species.

ACKNOWLEDGMENT

We thank Ms. Y. Ogata for technical assistance.

REFERENCES

1. Trounson A. Rats, cats and elephants, but still no unicorn: induced pluripotent stem cells from new species. Cell Stem Cell 2009; 4:3–4.
2. Aitman TJ, Critser JK, Cuppen E, Dominiczak A, Fernandez-Suarez XM, Flint J, Gauguier D, Geurts AM, Gould M, Harris PC, Holmdahl R, Hubner N, et al. Progress and prospects in rat genetics: a community view. Nat Genet 2008; 40:516–522.
3. Li P, Tong C, Mehrian-Shai R, Jia L, Wu N, Yan Y, Maxson RE, Schulze EN, Song H, Hsieh CL, Pera MF, Ying QL. Germline competent embryonic stem cells derived from rat blastocysts. Cell 2008; 135:1299–1310.
4. Buehr M, Meek S, Blair K, Yang J, Ure J, Silva J, McLay R, Hall J, Ying QL, Smith A. Capture of authentic embryonic stem cells from rat blastocysts. Cell 2008; 135:1287–1298.
5. Tong C, Li P, Wu NL, Yan Y, Ying QL. Production of p53 gene knockout rats by homologous recombination in embryonic stem cells. Nature 2010; 467:211–213.
6. Meistrich ML, van Beek MEAB. Spermatogonial stem cells. In: Desjardins CC, Ewing LL (eds.), Cell and Molecular Biology of the Testis. New York: Oxford University Press; 1993: 266–295.
7. Tegelenbosch RAJ, de Rooij DG. A quantitative study of spermatogonial multiplication and stem cell renewal in the C3H/101 F1 hybrid mouse. Mutat Res 1993; 290:193–200.
8. Brinster RL, Zimmermann JW. Spermatogenesis following male germ-cell transplantation. Proc Natl Acad Sci U S A 1994; 91:11298–11302.
9. Brinster RL, Avarbock MR. Germline transmission of donor haplotype following spermatogonial transplantation. Proc Natl Acad Sci U S A 1994; 91:11303–11307.
10. Kanatsu-Shinohara M, Shinohara T. The germ of pluripotency. Nat Biotechnol 2006; 24:663–664.
11. Kanatsu-Shinohara M, Ogonuki N, Inoue K, Miki H, Ogura A, Toyokuni S, Shinohara T. Long-term proliferation in culture and germline transmission of mouse male germline stem cells. Biol Reprod 2003; 69:612–616.
12. Meng X, Lindahl M, Hyvönen ME, Parvinen M, de Rooij DG, Hess MW, Raatikainen-Ahokas A, Sainio K, Rauvala H, Lakso M, Pichel JG, Westphal H, et al. Regulation of cell fate decision of undifferentiated spermatogonia by GDNF. Science 2000; 287:1489–1493.
13. Kanatsu-Shinohara M, Ogonuki N, Iwano T, Lee J, Kazuki Y, Inoue K, Miki H, Takehashi M, Toyokuni S, Shinkai Y, Oshimura M, Ishino F, et al. Genetic and epigenetic properties of mouse male germline stem cells during long-term culture. Development 2005; 132:4155–4163.
14. Liu X, Wu H, Loring J, Hormuzdi S, Disteche CM, Bornstein P, Jaenisch R. Trisomy eight in ES cells is a common potential problem in gene targeting and interferes with germ line transmission. Dev Dyn 1997; 209:85–91.
15. Longo L, Bygrave A, Grosveld FG, Pandolfi PP. The chromosome make-up of mouse embryonic stem cells is predictive of somatic and germ cell chimaerism. Transgenic Res 1997; 6:321–328.
16. Kanatsu-Shinohara M, Miki H, Inoue K, Ogonuki N, Toyokuni S, Ogura

A. Shinohara T. Long-term culture of mouse male germline stem cells under serum- or feeder-free conditions. Biol Reprod 2005; 72:985–991.
17. Kanatsu-Shinohara M, Toyokuni S, Shinohara T. Genetic selection of mouse male germline stem cells in vitro: offspring from single stem cells. Biol Reprod 2005; 72:236–240.
18. Kanatsu-Shinohara M, Ikawa M, Takehashi M, Ogonuki N, Miki H, Inoue K, Kazuki Y, Lee J, Toyokuni S, Oshimura M, Ogura A, Shinohara T. Production of knockout mice by random and targeted mutagenesis in spermatogonial stem cells. Proc Natl Acad Sci U S A 2006; 103:8018–8023.
19. Shinohara T, Kato M, Takehashi M, Lee J, Chuma S, Nakatsuji N, Kanatsu-Shinohara M, Hirabayashi M. Rats produced by interspecies spermatogonial transplantation in mouse and in vitro microinsemination. Proc Natl Acad Sci U S A 2006; 103:13624–13628.
20. Kanatsu-Shinohara M, Kato M, Takehashi M, Morimoto H, Takashima S, Chuma S, Nakatsuji N, Hirabayashi M, Shinohara T. Production of transgenic rats via lentiviral transduction and xenogeneic transplantation of spermatogonial stem cells. Biol Reprod 2008; 79:1121–1128.
21. Hamra FK, Gatlin J, Chapman KM, Grellhesl DM, Garcia JV, Hammer RE, Garbers DL. Production of transgenic rats by lentiviral transduction of male germ-line stem cells. Proc Natl Acad Sci U S A 2002; 99:14931–14936.
22. Ryu BY, Kubota H, Avarbock MR, Brinster RL. Conservation of spermatogonial stem cell self-renewal signaling between mouse and rat. Proc Natl Acad Sci U S A 2005; 102:14302–14307.
23. Hamra FK, Chapman KM, Nguyen DM, Williams-Stephens AA, Hammer RE, Garbers DL. Self-renewal, expansion, and transfection of rat spermatogonial stem cells in culture. Proc Natl Acad Sci U S A 2005; 102:17430–17435.
24. Izsvák Z, Fröhlich J, Grabundzija I, Shirley JR, Powell HM, Chapman KM, Ivics Z, Hamra FK. Generating knockout rats by transposon mutagenesis in spermatogonial stem cells. Nat Methods 2010; 7:443–445.
25. Friedrich G, Soriano P. Promoter traps in embryonic stem cells: a genetic screen to identify and mutate developmental genes in mice. Genes Dev 1991; 5:1513–1523.
26. Morita S, Kojima T, Kitamura T. Plat-E: an efficient and stable system for transient packaging of retroviruses. Gene Ther 2000; 7:1063–1066.
27. Kanatsu-Shinohara M, Inoue K, Miki H, Ogonuki N, Takehashi M, Morimoto T, Ogura A, Shinohara T. Clonal origin of germ cell colonies after spermatogonial transplantation in mice. Biol Reprod 2006; 75:68–74.
28. Fujihara Y, Murakami M, Inoue N, Satouh Y, Kaseda K, Ikawa M, Okabe M. Sperm equatorial segment protein 1, SPESP1, is required for fully fertile sperm in mouse. J Cell Sci 2010; 123:1531–1536.
29. Kanatsu-Shinohara M, Ogonuki N, Inoue K, Ogura A, Toyokuni S, Shinohara T. Restoration of fertility in infertile mice by transplantation of cryopreserved male germline stem cells. Hum Reprod 2003; 18:2660–2667.
30. Chuma S, Nakatsuji N. Autonomous transition into meiosis of mouse fetal germ cells in vitro and its inhibition by gp130-mediated signaling. Dev Biol 2001; 229:468–479.
31. Barrios F, Filipponi D, Pellegrini M, Paronetto MP, Di Siena S, Geremia R, Rossi P, De Fellici M, Jannini EA, Dolci S. Offspring effects of retinoic acid and FGF9 on Nanos2 expression and meiotic entry of mouse germ cells. J Cell Sci 2010; 123:871–880.
32. DiNapoli L, Batchvarov J, Capel B. FGF9 promotes survival of germ cells in the fetal testis. Development 2006; 133:1519–1527.
33. Lin FL, Sperle KM, Sternberg NL. Recombination in mouse L cells between DNA introduced into cells and homologous chromosomal sequences. Proc Natl Acad Sci U S A 1985; 82:1391–1395.
34. Smithies O, Gregg RG, Boggs SS, Koralewski MA, Kucherlapati RS. Insertion of DNA sequences into the human chromosomal beta-globin locus by homologous recombination. Nature 1985; 317:230–234.
35. Wurst W, Joyner AL. Production of targeted embryonic stem cell clones. In: Joyner AL (ed.), Gene Targeting. New York: Oxford University Press; 1993; 33–61.
36. te Riele H, Maandag ER, Berns A. Highly efficient gene targeting in embryonic stem cells through homologous recombination with isogenic DNA constructs. Proc Natl Acad Sci U S A 1992; 89:5128–5132.
37. Brinster RL, Brown RE, Lo D, Avarbock MR, Oram F, Palmiter RD. Targeted correction of a major histocompatibility class II E alpha gene by DNA microinjected into mouse eggs. Proc Natl Acad Sci U S A 1989; 86:7087–7091.
38. Orwig KE, Shinohara T, Avarbock MR, Brinster RL. Functional analysis of stem cells in the adult rat testis. Biol Reprod 2002; 66:944–949.
39. Danet GH, Pan Y, Luongo JL, Bonnet DA, Simon MC. Expansion of human SCID-repopulating cells under hypoxic conditions. J Clin Invest 2003; 112:126–135.
40. Takubo K, Goda N, Yamada W, Iriuchishima H, Ikeda E, Kubota Y, Shima H, Johnson RS, Hirao A, Suematsu M, Suda T. Regulation of the HIF-1 alpha level is essential for hematopoietic stem cells. Cell Stem Cell 2010; 7:391–402.
41. Ezashi T, Das P, Roberts RM. Low O_2 tensions and the prevention of differentiation of hES cells. Proc Natl Acad Sci U S A 2005; 102:4783–4788.
42. Biggers JD, Claringbold PJ. Why use inbred lines? Nature 1954; 174:596–597.
43. Richardson TE, Chapman KM, Terenhaus Dann C, Hammer RE, Hamra FK. Sterile testis complementation with spermatogonial lines restores fertility to *DazL*-deficient rats and maximizes donor germline transmission. PLoS One 2009; 4:e6308.
44. Ryu BY, Orwig KE, Oatley JM, Lin CC, Chang LJ, Avarbock MR, Brinster RL. Efficient generation of transgenic rats through the male germline using lentiviral transduction and transplantation of spermatogonial stem cells. J Androl 2007; 28:353–360.
45. Saitou M, Furuse M, Sasaki H, Schulzke JD, Fromm M, Takano H, Noda T, Tsukita S. Complex phenotype of mice lacking occludin, a component of tight junction strands. Mol Biol Cell 2000; 11:4131–4142.
46. Kanatsu-Shinohara M, Inoue K, Ogonuki N, Morimoto H, Ogura A, Shinohara T. Serum- and feeder-free culture of mouse germline stem cells. Biol Reprod 2011; 84:97–105.
47. Ludwig TE, Levenstein ME, Jones JM, Berggren WT, Mitchen ER, Frane JL, Crandall LJ, Daigh CA, Conard KR, Piekarczyk MS, Lianas RA, Thomson JA. Derivation of human embryonic stem cells in defined conditions. Nat Biotechnol 2006; 24:185–187.
48. Wakayama T, Perry AC, Zuccotti M, Johnson KR, Yanagimachi R. Full-term development of mice from enucleated oocytes injected with cumulus cell nuclei. Nature 1998; 394:369–374.
49. Aponte PM, Soda T, Teerds KJ, Mizrak SC, van de Kant HJ, de Rooij DG. Propagation of bovine spermatogonial stem cells in vitro. Reproduction 2008; 136:543–557.
50. Kanatsu-Shinohara M, Muneto T, Lee J, Takenaka M, Chuma S, Nakatsuji N, Horiuchi T, Shinohara T. Long-term culture of male germline stem cells from hamster testes. Biol Reprod 2008; 78:611–617.
51. Sadri-Ardekani H, Mizrak SC, van Daalen SK, Korver CM, Roepers-Gajadien HL, Koruji M, Hovingh S, de Reijke TM, de la Rosette JJ, van der Veen F, de Rooij DG, Repping S, et al. Propagation of human spermatogonial stem cells in vitro. JAMA 2009; 302:2127–2134.

OPEN ACCESS Freely available online

PLoS one

Dynamic Changes in EPCAM Expression during Spermatogonial Stem Cell Differentiation in the Mouse Testis

Mito Kanatsu-Shinohara[1], Seiji Takashima[1], Kei Ishii[1], Takashi Shinohara[1,2]*

1 Department of Molecular Genetics, Graduate School of Medicine, Kyoto University, Kyoto, Japan, **2** Japan Science and Technology Agency, CREST, Kyoto, Japan

Abstract

Background: Spermatogonial stem cells (SSCs) have the unique ability to undergo self-renewal division. However, these cells are morphologically indistinguishable from committed spermatogonia, which have limited mitotic activity. To establish a system for SSC purification, we analyzed the expression of SSC markers CD9 and epithelial cell adhesion molecule (EPCAM), both of which are also expressed on embryonic stem (ES) cells. We examined the correlation between their expression patterns and SSC activities.

Methodology and Principal Findings: By magnetic cell sorting, we found that EPCAM-selected mouse germ cells have limited clonogenic potential in vitro. Moreover, these cells showed stronger expression of progenitor markers than CD9-selected cells, which are significantly more enriched in SSCs. Fluorescence-activated cell sorting of CD9-selected cells indicated a significantly higher frequency of SSCs among the $CD9^{+}EPCAM^{low/-}$ population than among the $CD9^{+}EPCAM^{+}$ population. Overexpression of the active form of EPCAM in germline stem (GS) cell cultures did not significantly influence SSC activity, whereas EPCAM suppression by short hairpin RNA compromised GS cell proliferation and increased the concentration of SSCs, as revealed by germ cell transplantation.

Conclusions/Significance: These results show that SSCs are the most concentrated in $CD9^{+}EPCAM^{low/-}$ population and also suggest that EPCAM plays an important role in progenitor cell amplification in the mouse spermatogenic system. The establishment of a method to distinguish progenitor spermatogonia from SSCs will be useful for developing an improved purification strategy for SSCs from testis cells.

Citation: Kanatsu-Shinohara M, Takashima S, Ishii K, Shinohara T (2011) Dynamic Changes in EPCAM Expression during Spermatogonial Stem Cell Differentiation in the Mouse Testis. PLoS ONE 6(8): e23663. doi:10.1371/journal.pone.0023663

Editor: Renee A. Reijo Pera, Stanford University, United States of America

Received May 5, 2011; **Accepted** July 22, 2011; **Published** August 15, 2011

Funding: Financial support for this research was supported by the Genome Network Project, Japan Science and Technology Agency (CREST), Program for Promotion of Basic and Applied Researches for Innovation in Bio-orientated Industry, the Ministry of Health, Labour, and Welfare, The Cabinet Office, Government of Japan through its "Funding Program for Next Generation World-Leading Researchers," and the Ministry of Education, Culture, Sports, Science, and Technology (MEXT). The funders had no role in study design, data collection and analysis, decision to publish, or preparation of the manuscript.

Competing Interests: The authors have declared that no competing interests exist.

* E-mail: takashi@mfour.med.kyoto-u.ac.jp

Introduction

Spermatogonial stem cells (SSCs) account for a small population of testis cells [1,2], and their self-renewal activity distinguishes them from committed progenitor cells. Spermatogonia, the most undifferentiated germ cells in testes, contain both SSCs and progenitor cells. SSCs are able to reproduce themselves while producing progenitor cells, thereby maintaining a constant population size. In contrast, progenitor spermatogonia disappear after several rounds of mitotic division. Self-renewal activity is defined only through retrospective analysis of daughter cells, making it difficult or impossible to identify SSCs by morphological observation.

In 1994, a germ cell transplantation technique was developed, in which donor testis cells recolonize seminiferous tubules following microinjection into the testes of infertile recipients [3]. This provided the first functional assay for SSCs. The estimated number of SSCs was 2×10^3 to 3×10^3 per testis, which represents ~10% of the total A_{single} (A_s) spermatogonia, suggesting that only a small population of A_s cells have SSC activity [2,4,5]. Using the functional transplantation assay, SSCs were subsequently analyzed for the expression of cell surface markers by selecting cells with monoclonal antibodies against surface antigens [6,7]. Although no SSC-specific markers have been identified, several markers for SSCs are available [8], and a combination of positive and negative selection by surface antigens has allowed the purification of SSCs to 1 in 15 to 30 purified cells [6,7]. However, the degree of enrichment achieved using individual antigens is limited and ranges from 1:625 to 1:1250 [6–8], suggesting that committed spermatogonia express similar markers.

In this study, we analyzed the expression of CD9 and epithelial cell adhesion molecule (EPCAM) on SSCs. CD9 is a member of the tetraspanin family molecules and is expressed on mouse and rat SSCs [9]. On the other hand, EPCAM is a homophilic, calcium-independent cell adhesion molecule and is uniquely expressed on the germline cells from the embryonic stages of germ cell development. Its expression in the postnatal testis continues until the spermatocyte stage [10]. Although both of

these antigens have been used to purify SSCs, EPCAM was the more useful marker for purifying rat SSCs [11]. However, while attempting to initiate SSC cultures from mouse testes, we observed that EPCAM-expressing cells had limited ability to produce spermatogonial colonies. Flow cytometric analysis revealed that EPCAM expression changed dynamically during spermatogonial differentiation. Here, the identity of EPCAM-expressing cells was determined by germ cell transplantation assay, and the function of EPCAM was analyzed by in vitro spermatogonial culture.

Materials and Methods

Ethics statement

We followed the Fundamental Guidelines for Proper Conduct of Animal Experiment and Related Activities in Academic Research Institutions under the jurisdiction of the Ministry of Education, Culture, Sports, Science and Technology, and all of the protocols for animal handling and treatment were reviewed and approved by the Animal Care and Use Committee of Kyoto University (Med Kyo 11079).

Animals

ICR mice (Japan SLC, Shizuoka, Japan) were used for primary testis cell culture. Transgenic mouse line C57BL/6 Tg14(act-EGFP)OsbY01 (designated as Green; a gift from Dr. M. Okabe, Osaka University, Osaka, Japan) was used for transplantation experiments using magnetic cell sorting (MACS). Transgenic mouse line B6-TgR(ROSA26)26Sor (designated as ROSA; purchased from the Jackson Laboratory, Bar Harbor, ME) was used for fluorescence-activated cell sorting (FACS) experiments to avoid interference of enhanced green fluorescent protein (EGFP) fluorescence for multiparameter sorting. ROSA mice that were backcrossed to the DBA/2 background for more than eight generations were used for derivation of germline stem (GS) cells [12]. WBB6F1-W/W^{v} (W) mice (Japan SLC) were used as recipients for germ cell transplantation.

Cell culture

For characterization of spermatogonia in the pup testis, testis cells were prepared from 7- to 10-day-old male mice. Single-cell suspensions were obtained by two-step enzymatic digestion using collagenase type IV (1 mg/ml) and trypsin (0.25%), as described previously [12,13]. Cells were plated at 3×10^5 cells / well of 6-well culture plates, which have been coated with laminin (20 μg/ml; BD Biosciences, Franklin Lakes, NJ). GS cells were derived from ROSA mice, and were maintained on mitomycin C-treated mouse embryonic fibroblasts (MEFs) [12,13]. Culture medium was prepared by modifying commercial medium (StemPro®-34 serum-free medium (SFM); Invitrogen, Carlsbad, CA) as described previously [12,13]. Growth factors used were human fibroblast growth factor 2 (FGF2;10 ng/ml) and rat glial cell line-derived neurotrophic factor (GDNF; 15 ng/ml; both from Peprotech, Rocky Hill, NJ).

For overexpression of the intracellular fragment of EPCAM (EpICD) [14], the cDNA fragment encoding EpICD (a gift from Dr. O. Gires, Ludwig Maximilian University of Munich, Germany) was cloned into *CSII-EF-IRES2-Venus* vector. Lentivirus particles were produced by transient transfection of 293T cells, and GS cells from ROSA mice (ROSA GS cells) were transfected, as described previously [15]. For EpICD overexpression experiments, the virus titer was determined by transfecting 293T cells, and the multiplicities of infection (MOI) was adjusted to 2.0. For short hairpin RNA (shRNA)-mediated gene knockdown (KD), the *Epcam* KD vectors TRCN0000111220, TRCN0000111221, TRCN0000111222, TRCN0000111223, and TRCN0000111224 were purchased from Open Biosystems (Huntsville, AL). A mixture of lentivirus particles was used to transfect GS cells from ROSA mice, and 3 independent samples were examined. A lentivirus expressing shRNA against EGFP was used as a control (Open Biosystems). The lentivirus titer was determined using a Lenti-X p24 rapid titer kit (Clontech, Mountain View, CA). The MOI in the KD experiment was adjusted to 24.0.

Cell separation and flow cytometry

Testis cells were prepared from 5- to 10-week-old male mice. MACS was performed as described previously using rat anti-mouse EPCAM (G8.8; Biolegend, San Diego, CA) or rat anti-mouse CD9 (KMC8; BD Biosciences) antibodies [9,16]. Sheep anti-rat IgG Dynabeads (Invitrogen) were used for in vitro culture, and goat anti-rat IgG microbeads (Miltenyi Biotech, Gladbach, Germany) were used as a secondary antibody for FACS experiments. The average recovery was determined by four experiments.

For analyses of cell surface antigens, CD9- or EPCAM-selected cells were incubated with the following antibodies: rat anti-mouse CD9 (2B8; BD Biosciences), rat anti-mouse EPCAM (G8.8; Biolegend), mouse anti-mouse FUT4 (SSEA1; MC-480; eBioscience, San Diego, CA), biotin-conjugated anti-mouse ITGB1 (Ha2/5; BD Biosciences), and rat anti-mouse ITGA6 (GoH3; BD Biosciences). Secondary reagents were: allophycocyanin (APC)-conjugated anti-rat IgG, APC-conjugated streptavidin, and APC-conjugated anti-mouse IgM (all from BD Biosciences). For double immunostaining, CD9-selected cells were incubated with APC-conjugated rat ant-CD9 and phycoerythrin (PE)-conjugated anti-EPCAM antibodies. PE-Cy7-conjugated KIT antibody (eBioscience) was used to evaluate KIT expression in subfractionated cells. The cells were incubated in ice-cold phosphate-buffered saline/1% fetal bovine serum (PBS/1% FBS). EpICD-transfected ROSA GS cells were sorted according to Venus expression. Propidium iodide (1 μg/ml; Sigma, St. Louis, MO) was added to exclude dead cells. Stained cells were analyzed by FACSCalibur or sorted by FACSAria II (both from BD Biosciences).

Apoptosis assay

For terminal deoxynucleotidyl transferase dUTP nick end labeling (TUNEL) staining, single cell suspension was concentrated on glass slides by centrifugation with Cytospin 4 (Thermo Electron Corporation, Cheshire, UK). After fixation in 4% paraformaldehyde for 1 h, cells were then labeled using an In situ Cell Death Detection kit; TMR red (Roche Applied Science, Mannheim, Germany) following the manufacturer's protocol. The cells were couterstained with Hoechst 33342 (2 μg/ml; Sigma) to determine the percentage of TUNEL-positive nuclei relative to the total number of cells. Apoptotic cells were quantified by collecting three images using Photoshop software (Adobe Systems, San Jose, CA). At least 200 cells were counted for each sample.

Germ cell transplantation

Germ cell transplantation was performed by microinjection into the seminiferous tubules via the efferent duct [17]. Approximately 75–85% of the tubules were filled in each recipient testis. At least three experiments were carried out for MACS and FACS. In experiments using GS cells, recipient mice were treated with anti-CD4 antibody (GK1.5; gift from Dr. T. Honjo, Kyoto University) to avoid rejection of allogeneic donor cells [18]. The Institutional Animal Care and Use Committee of Kyoto University approved all of the animal experiment protocols.

Analysis of the recipient testes

In experiments using ROSA mice, the recipient testes were fixed with 4% paraformaldehyde for 2 h, and LacZ staining was performed using 5-bromo-4-chloro-3-indolyl ß-D-galactoside (X-Gal) (Wako Pure Chemical Industries, Osaka, Japan), as described previously [5]. In experiments using Green mice, the recipient testes were analyzed under UV light. These methods specifically identify donor cells, because host cells do not stain for LacZ and lack green fluorescence. We defined colonies as donor cell clusters longer than 0.1 mm occupying the entire circumference of the seminiferous tubule. Results were obtained from analyses of 10–12 recipient testes in at least two experiments. For histological analyses, samples were embedded in paraffin blocks and sectioned. The sections were counterstained with hematoxylin and eosin.

Analysis of gene expression

Total RNA was extracted using Trizol, and first-strand cDNA was synthesized by reverse transcription with Superscript™ II (both from Invitrogen) for reverse transcriptase-polymerase chain reaction (RT-PCR). For quantifying mRNA expression using real-time PCR, a StepOnePlus™ Real-Time PCR system and *Power* SYBR Green PCR Master Mix were used according to the manufacturer's protocol (Applied Biosystems, Warrington, UK). Transcript levels were normalized to that of *Hprt*, with expression levels in EPCAM-selected cells. The PCR conditions were 95°C for 10 min, followed by 40 cycles of 95°C for 15 s and 60°C for 1 min. Each PCR was run at least in triplicate using specific primers (Table S1).

Statistical analysis

The results were presented as means±SEM. Independent samples with equal variance were analyzed using the Student's *t*-test. SSC activity of subfractionated cells was analyzed by ANOVA followed by Tukey's HSD.

Results

Reduced SSC potential of EPCAM $^{+}$ cells

Testicular somatic cells often overwhelm growth of proliferating germ cells in vitro [12]. To establish an improved strategy for SSC culture initiation, we assumed that EPCAM would be a useful selection marker because it is thought to be expressed specifically in germ cells, including SSCs [8,10]. In preliminary experiments, we used anti-EPCAM antibody to collect EPCAM-expressing germ cells from pup testes, which are relatively enriched for SSCs owing to the absence of differentiating germ cells [19]. Testis cells were prepared from 7-day-old pups, and EPCAM-expressing cells were collected by MACS. The cells were cultured on laminin-coated plates. Although CD9-selected cells contained testicular somatic cells that over-proliferated and interfered with germ cell proliferation in culture, the majority of the EPCAM-selected cells consisted of a pure population of germ cells; only a few somatic cells were found (Fig. 1A). However, proliferation of the EPCAM-selected cells was limited, and many of the cells eventually underwent apoptosis, which was identified by TUNEL staining (5.0±0.8% vs. 28.7±0.4%, respectively, for CD9- and EPCAM-selected cells; Fig. 1B). In contrast, cultures initiated with CD9-selected cells exhibited typical spermatogonial proliferation and colony growth by 7–10 days.

As these results indicated that EPCAM-selected cells have limited clonogenic potential in vitro, we characterized the EPCAM- and CD9-selected cells. EPCAM- and CD9-expressing cells were collected by MACS and stained for several cell surface markers known to be expressed on germline cells [8,20] (Fig. 1C). Although both EPCAM- and CD9-selected cells expressed markers of SSCs, expression of KIT, which is a marker for progenitor spermatogonia [20], was stronger in EPCAM-selected cells, which suggested that they included more progenitor spermatogonia. In addition, CD9-selected cells also contained a significant proportion of cells that did not express EPCAM. Real-time PCR analysis of genes thought to be involved in SSC self-renewal and differentiation revealed reduced expression of *Nanos3*, *Bcl6b*, and *Etv5* in EPCAM-selected cells [8,21–23] (Fig. 1D). The expression levels of *Ccnd1* and *Ccnd2*, which influence SSC activity [24], were also downregulated. These results suggest that EPCAM-selected cells have reduced SSC activity.

To directly test this hypothesis, EPCAM- or CD9-expressing cells were collected and their SSC activities were assessed by germ cell transplantation. The average recoveries of EPCAM- and CD9-selected cells were 4.9±1.0% and 5.9±0.5% of the total testis cells, respectively. The selected cells were microinjected into the seminiferous tubules of congenitally infertile W mouse testes. Two months later, the recipients were killed, and the number of colonies in the testes was analyzed under UV fluorescence (Fig. 1E). EPCAM-selected cells produced significantly more colonies compared with non-selected control cells (5.7±1.0 vs. 1.9±0.4 colonies/10^5 transplanted cells, respectively; Fig. 1F). In contrast, in two transplantation experiments, the CD9-selected cells resulted in more efficient SSC recovery, producing 29.5±2.3 colonies/10^5 transplanted cells, which was 32.8 times the number of colonies from the control cells (0.9±0.6 colonies). These experiments suggest that the concentration of SSCs is higher among CD9-selected cells than EPCAM-selected cells.

Subfractionation of CD9-selected cells by EPCAM expression level

To investigate the difference between EPCAM- and CD9-selected cells in the transplantation experiments, we next analyzed the expression of EPCAM and CD9 in EPCAM- and CD9-selected cells of ROSA mice recovered by MACS. Flow cytometry of the double-stained spermatogonial populations was performed by gating according to cell size (forward scatter) and complexity (side scatter). As expected from the result of MACS experiments, CD9-selected cells contained cells with relatively high side scatter values, which suggested their heterogeneity (Fig. 2A). In contrast, EPCAM-selected cells were more uniform in size and complexity. Double-stained CD9-selected cells revealed the presence of at least three subpopulations (Fig. 2B). Fraction I consisted of cells exhibiting strong CD9 expression with relatively weak EPCAM expression. Fraction II, which contained significantly more cells than fraction I, comprised cells with strong EPCAM expression and medium CD9 expression. A CD9$^{low/-}$ population of cells that lacked EPCAM constituted fraction III. Compared with the CD9-selected cells, the EPCAM-selected cells showed a distinct forward scatter/side scatter profile and consisted predominantly of fraction II cells. They also contained only EPCAM^{-} cells of fraction I cells (Fig. 2A). KIT expression was stronger in fraction II than in fraction I cells, suggesting that fraction I cells were more undifferentiated (Fig. 2C). Fraction III showed little KIT expression (Fig. 2C).

We then analyzed testis cells from three different developmental stages to examine when these subpopulations appear during testicular development. We collected testis cells from 1-, 10-, and 35-day-old mice and stained them with CD9 and EPCAM antibodies (Fig. 2D). Testis cells from 1-day-old mice contained only gonocytes, and showed predominantly CD9^{+} cells, with very few EPCAM^{+} cells. EPCAM^{+} cells were found in 10-day-old mouse testis cells, which contained spermatogonia and spermatocytes, but

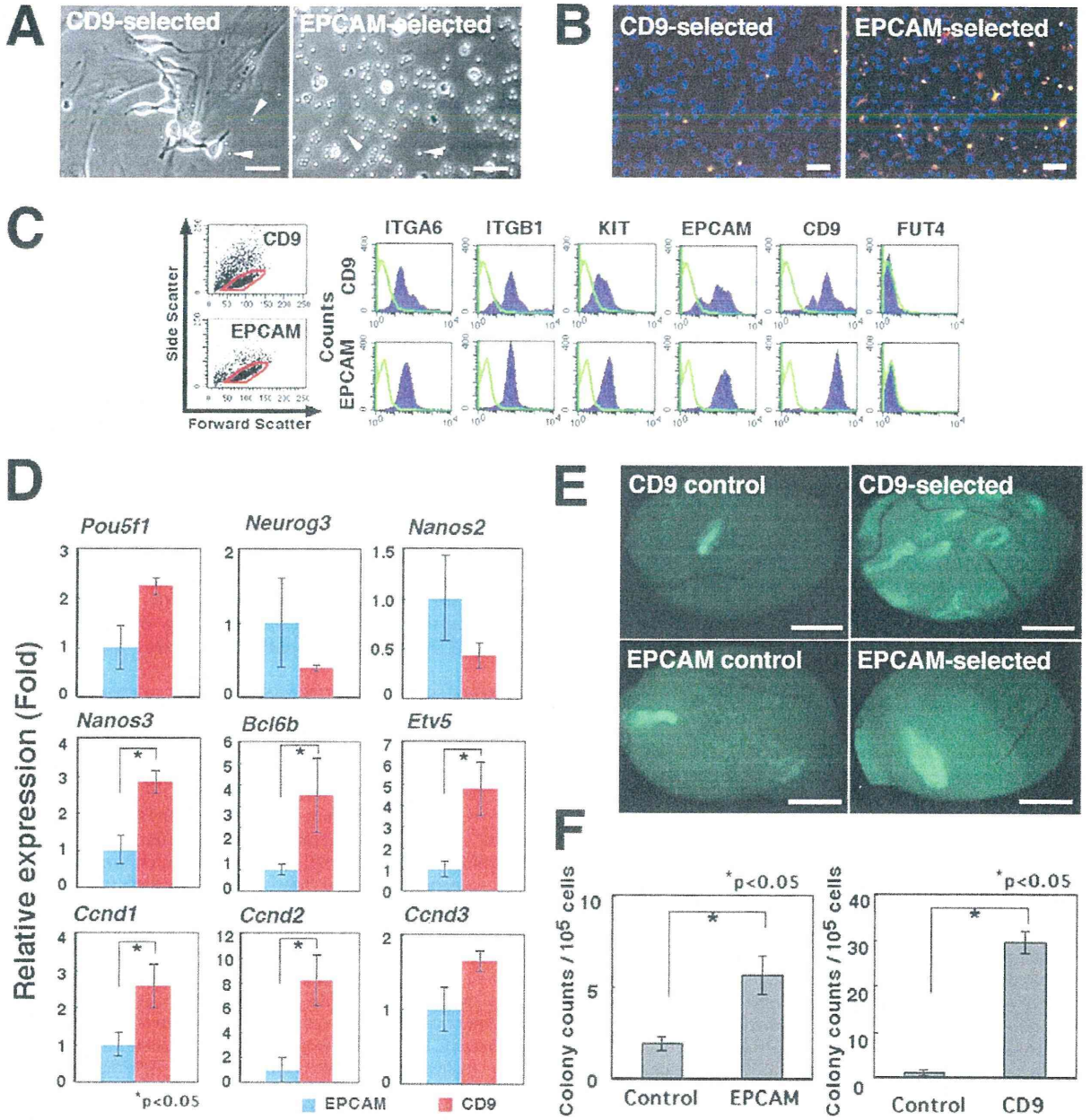

Figure 1. Characteristics of germ cells after CD9 or EPCAM selection. (A) Appearance of CD9-selected (Left) or EPCAM-selected (Right) germ cells on laminin-coated dishes, after 7 days in culture. Testis cells were collected from 10-day-old pups and used to initiate GS cell cultures after MACS. No significant colony formation is seen in EPCAM-selected cells. CD9-selected cells started to proliferate to form spermatogonia chains under the same culture condition, and spermatogonial chains are seen. Note the contaminating testicular fibroblasts in cultures of CD9-selected cells. Arrows indicate magnetic beads used for cell separation. (B) Apoptosis of CD9-selected (Left) and EPCAM-selected cells (Right), after 8 days in culture. TUNEL-positive cells are stained red. Counterstained by Hoechst 33342 (blue). (C) Flow cytometric analyses of CD9-selected (Top) or EPCAM-selected (Bottom) cells collected from adult testes. Green lines indicate control staining. Note the increased KIT staining in EPCAM-selected cells. (D) Real-time PCR analyses of spermatogonial marker genes or cyclins in EPCAM- or CD9-selected cells. CD9-selected cells show increased expression of *Nanos3, Bcl6b, Etv5, Ccnd1*, and *Ccnd2*. Transcript levels were normalized to *Hprt* expression, with expression levels in EPCAM-selected cells. (E) Macroscopic appearance of recipient testes transplanted with EPCAM- or CD9-selected cells. Green tubules indicate germ cell colonies developed from donor SSCs. The same numbers of cells were transplanted at the same time. (F) Quantification of colonies. Both EPCAM-selected (Left) and CD9-selected (Right) cells produced significantly more germ cell colonies than control unselected testis cells, but CD9-selected cells contained a higher concentration of SSCs. Bars = 20 μm (A); 100 μm (B); 1 mm (E).
doi:10.1371/journal.pone.0023663.g001

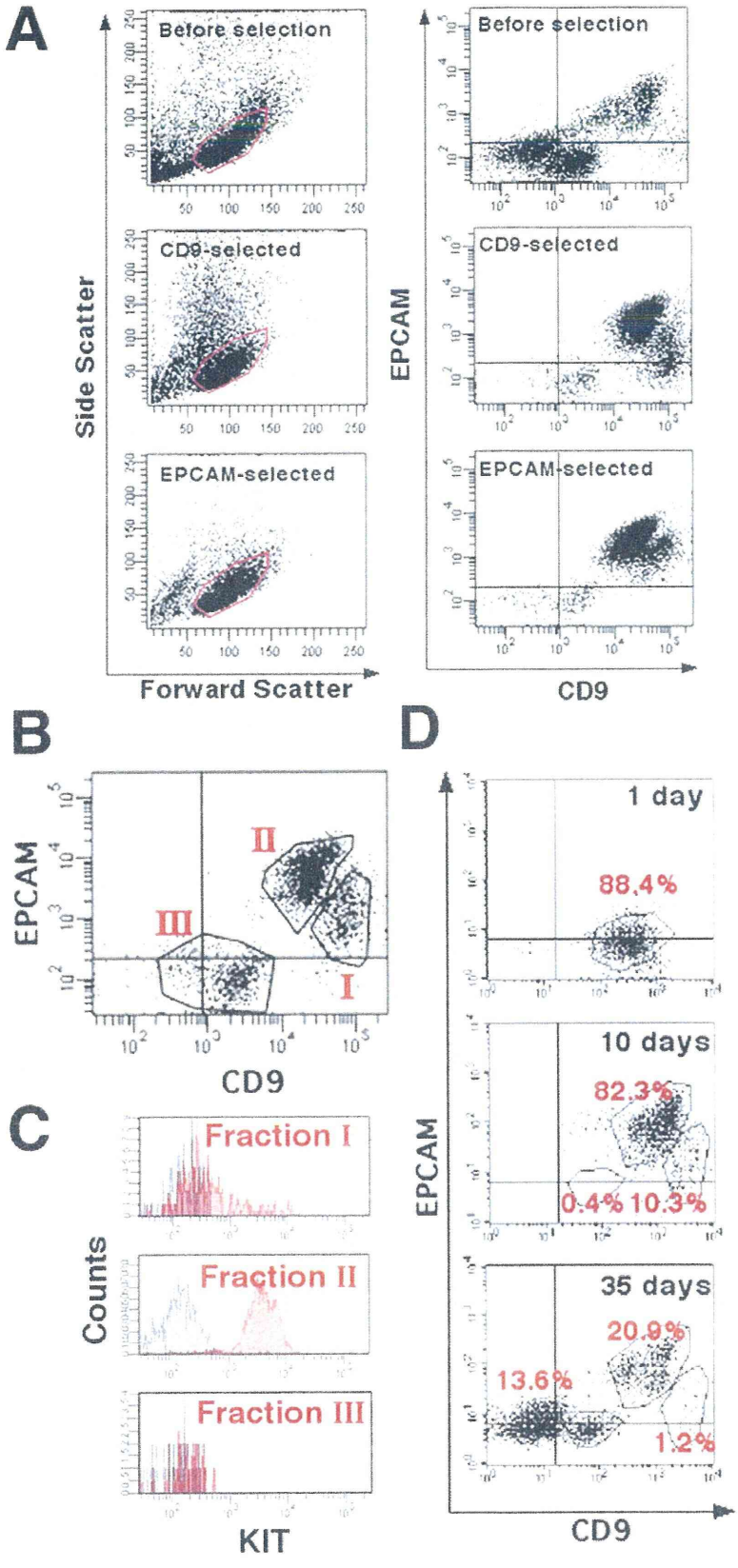
A
Before selection
CD9-selected
EPCAM-selected
Side Scatter
Forward Scatter
EPCAM
CD9
B
EPCAM
CD9
II
III
I
C
Fraction I
Fraction II
Fraction III
Counts
KIT
D
1 day
88.4%
10 days
82.3%
0.4%
10.3%
35 days
20.9%
13.6%
1.2%
EPCAM
CD9

Figure 2. Flow cytometric analyses of CD9- or EPCAM-selected cells after MACS. (A) Light-scattering properties and double immunostaining of total testis cells (Top), CD9-selected cells (Middle) or EPCAM-selected cells (Bottom) stained with APC-conjugated anti-CD9 and PE-conjugated anti-EPCAM antibodies. Cells were gated according to forward scatter (size) and side scatter (cell complexity) values (Left). Gated cells were analyzed for CD9 and EPCAM (Right). Note the simpler light-scattering properties of EPCAM-selected cells. (B) Three subpopulations of CD9-selected cells. Fraction I shows high CD9 and low or no EPCAM immunostaining; fraction II shows low CD9 and high EPCAM immunostaining; and fraction III is low or no CD9 and no EPCAM immunostaining. (C) The three CD9-selected cell subpopulations, immunostained with APC-conjugated anti-CD9, PE-conjugated anti-EPCAM, and PE-Cy7-conjugated anti-KIT antibodies. KIT is strongly expressed in fraction II. Areas shaded in black indicate control staining. (D) Changes in immunostaining of total testis cells during postnatal testicular development. Total testis cells were stained with APC-conjugated anti-CD9 and PE-conjugated anti-EPCAM antibodies. Stronger CD9 and EPCAM immunostaining is seen in 10-day-old mouse testis cells compared with 1-day-old mouse testis cells. Only testes from 35-day-old mice show all three fractions.
doi:10.1371/journal.pone.0023663.g002

not spermatids. Testis cells at this stage could be separated into two subpopulations, fraction I ($CD9^{-}EPCAM^{low/-}$) and fraction II ($CD9^{low}EPCAM^{+}$), with fraction I being significantly smaller. Testis cells from 35-day-old mice contained all stages of spermatogenic cells, and revealed three subpopulations; the relative proportion of cells in fraction I was smaller than that in 10-day-old mouse testis cells, possibly reflecting increased production of differentiating meiotic or haploid cells. These results suggest an enrichment of fraction I ($CD9^{-}EPCAM^{low/-}$) in spermatogonia.

To determine which CD9-selected cell fraction was enriched for SSCs, cells from each of the three fractions were transplanted into the seminiferous tubules of recipient mice. Non-selected total testis cells were used as a control. Fraction I cells exhibited the highest SSC activity in recipient testes, producing 86.6±24.4 colonies/10^5 transplanted cells (Fig. 3A and B). The concentration of SSCs in this fraction was ~48.7-fold that in control cells, which produced 1.8±0.5 colonies/10^5 transplanted cells. Consistent with this result, microscopic analysis of the sorted cells showed that fraction I consisted of cells with a relatively uniform appearance and occasional pseudopod formation (Fig. 3A, inset). Histological sections confirmed the normal appearance of the transplanted cells (Fig. 3C). Although fraction II also contained some SSCs (1.1±0.6 colonies/10^5 cells transplanted), no significant enrichment was observed compared with non-selected control testis cells. Fraction III cells had no SSC activity.

Analysis of EPCAM function

To investigate the function of EPCAM, we used the GS cell culture system, in which SSCs increase their numbers exponentially in vitro in the presence of GDNF and FGF2 [12]. GS cells were previously shown to express EPCAM, and 1–2% of GS cells had SSC activity [12,25]. Flow cytometric analyses showed that the EPCAM expression level in GS cells was upregulated by supplementation with GDNF, whereas FGF2 showed no apparent effect (Fig. 4A).

Considering the expression of EPCAM on embryonic stem (ES) cells and rat SSCs, we examined whether stimulation of EPCAM increases SSC activity. GS cells from ROSA mice were infected

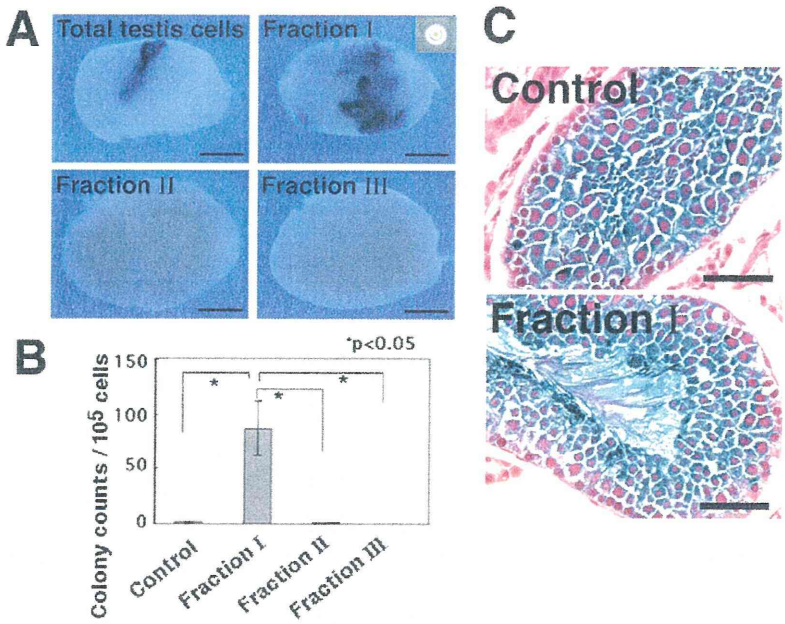

Figure 3. Functional analyses of SSC activity by germ cell transplantation of each CD9-selected cell fraction. (A) Macroscopic appearance of recipient testes. Approximately 4.9×10^3, 2.3×10^4, 3.5×10^2, and 1.6×10^5 cells were transplanted for fractions I, II, III, and control cells, respectively. Recipient testes were stained with X-Gal 2 months after transplantation. Blue tubules indicate germ cell colonies developed from donor SSCs. Cells in fraction I have a uniform appearance (insert). (B) Quantification of colonies. The number of cells that could be recovered in each experiment varied, and thus the colony number was normalized to reflect donor cells at a concentration of 10^5 cells injected/testis. Cells in fraction I are significantly enriched for SSCs. (C) Histological sections of recipient testes. Note the normal appearance of spermatogenesis of donor-derived cells in recipients of control cells (Top) and fraction I cells (Bottom). Stain: X-Gal (A); X-Gal, Hematoxylin and eosin (C). Bars = 1 mm (A), 50 μm (C).
doi:10.1371/journal.pone.0023663.g003

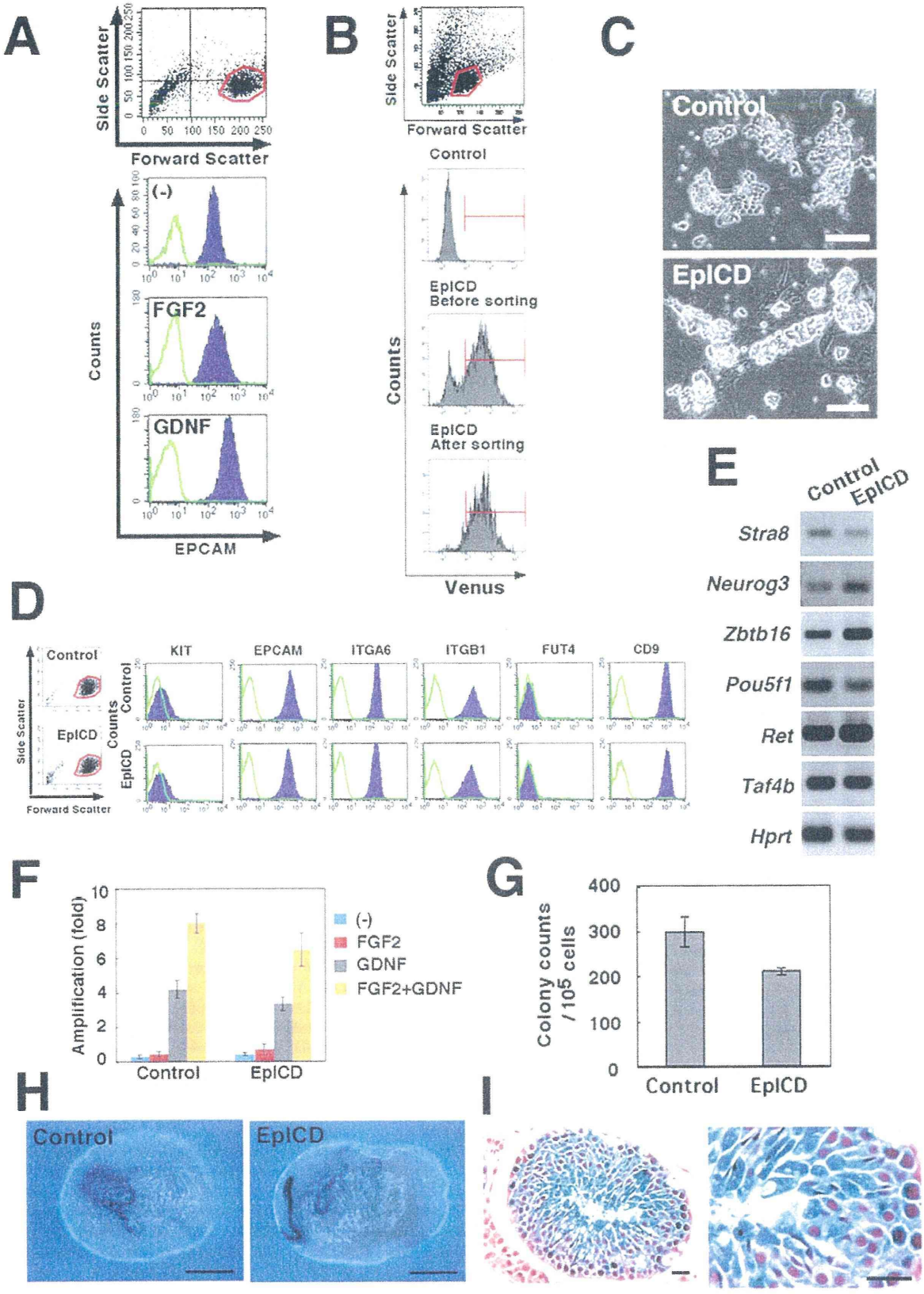
A
Side Scatter
Forward Scatter
(-)
FGF2
GDNF
Counts
EPCAM
B
Side Scatter
Forward Scatter
Control
EpICD
Before sorting
EpICD
After sorting
Counts
Venus
C
Control
EpICD
D
Control
EpICD
Side Scatter
Forward Scatter
Counts
KIT
EPCAM
ITGA6
ITGB1
FUT4
CD9
E
Control
EpICD
Stra8
Neurog3
Zbtb16
Pou5f1
Ret
Taf4b
Hprt
F
Amplification (fold)
(-)
FGF2
GDNF
FGF2+GDNF
Control
EpICD
G
Colony counts / 10^5 cells
Control
EpICD
H
Control
EpICD
I

Figure 4. Overexpression of EpICD in ROSA GS cells. (A) Upregulation of EPCAM by GDNF stimulation. ROSA GS cells were cultured on laminin with 1% FBS and without cytokines for 3 days and then stimulated with the indicated cytokines. The cells were recovered 3 days after cytokine stimulation, and stained with anti-EPCAM antibody. (B) Sorting of EpICD-transfected GS cells. GS cells (3×10^5) on MEFs in 6-well plates were infected, expanded in vitro, and sorted. (C) Morphology of the sorted cells. (D, E) Flow cytometric (D) and RT-PCR (E) analyses of EpICD-transfected ROSA GS cells. No significant changes are seen. Green lines indicate controls. (F) Effects of cytokines on proliferation of EpICD-transfected ROSA GS cells. GS cells (3×10^5) on MEFs were cultured with the indicated cytokines and recovered by trypsinization 6 days after initiation of culture. No significant differences are seen between the control and EpICD-transfected cells. (G) Quantification of colonies. No significant differences are seen between the control and EpICD-transfected cells. (H) Macroscopic appearance of recipient testes. Recipient testes were stained with X-Gal 2 months after transplantation. Blue tubules indicate germ cell colonies developed from donor SSCs. (I) Histological sections of recipient testes. Cells show apparently normal spermatogenesis. Stain: X-Gal (H); X-Gal, Hematoxylin and eosin (I). Bars = 100 μm (C), 1 mm (H), 20 μm (I).
doi:10.1371/journal.pone.0023663.g004

with a lentivirus expressing the intracellular domain of EPCAM (EpICD) as well as Venus protein under the control of the *EF-1* αpromoter. Normally in cells, EpICD is normally cleaved after EPCAM activation, and thus the EpICD protein can transmit the signal to the nucleus. *Venus*-expressing cells were purified and cultured in vitro for expansion (Fig. 4B and C). However, the transfected cells did not undergo a significant change in cell or colony morphology (Fig. 4C). In addition, flow cytometric analyses showed no change in the expression level of EPCAM or any other spermatogonial marker examined (Fig. 4D). There were no significant changes in gene expression patterns as determined by RT-PCR or in responses to exogenous cytokines (Fig. 4E and F) [8,26].

To look at the effect of EPCAM stimulation on SSC self-renewal, we transplanted EpICD-expressing GS cells into seminiferous tubules in two experiments. LacZ staining of the recipient testes showed that the numbers of colonies generated from EpICD-GS and control GS cells were 210.4±8.4 and 298.1±34.1/10^5 transplanted cells, respectively. The value for EpICD-GS cells was not significantly different from control value (Fig. 4G and H). Histological analysis of the recipient testes showed normal spermatogenesis (Fig. 4I). Thus, overexpression of EpICD did not appear to change SSC activity.

In the second set of experiments, we used shRNA to inhibit EPCAM expression. Transfection of ROSA GS cells with *Epcam* KD lentivirus vector significantly suppressed EPCAM expression within 2 days (Fig. 5A and B). EPCAM downregulation suppressed the proliferation/survival of GS cells (Fig. 5C). Only 30.4±7.6% of the input cells were recovered after *Epcam* KD treatment, whereas 73.8±8.8% of the input cells could be recovered after control shRNA treatment. These results indicate that EPCAM plays a role in the proliferation or survival of GS cells.

We next evaluated the SSC activity by transplanting the *Epcam* KD-transfected cells into the seminiferous tubules. Two days after infection, the cultured cells were transplanted into the testes of W mice. In two separate experiments, *Epcam* KD cells and control GS cells generated 1.6±0.5 and 0.1±0.1 colonies/10^5 transplanted cells, respectively; the difference was statistically significant (Fig. 5D and E). Thus, the *Epcam* KD treatment increased the concentration of SSCs in GS cell cultures.

Discussion

Although EPCAM has been considered as a homophilic cell adhesion molecule, a series of recent studies has shown that EPCAM, upon cleavage into small fragments, transmits proliferation signals [14,27,28]. The short intracellular domain EpICD binds to a scaffolding protein, four-and-a-half LIM domains protein 2, and is translocated into the nucleus, where it becomes part of a large nuclear complex containing CTNNB1 and LEF1, two components of the Wnt pathway. This causes upregulation of MYC and cyclins, thereby facilitating proliferation. Consistent with this, *Epcam* KD compromised proliferation of embryonic stem (ES) cells [29]. EPCAM is also closely related to the maintenance of the undifferentiated state; EPCAM was downregulated by leukemia inhibitory factor (LIF) withdrawal, and KD treatment led to extensive differentiation [29]. As exogenously expressed EPCAM could only partially compensate for the requirement of ES cells for LIF, EPCAM is considered to be essential, but not sufficient for maintenance of the ES cell phenotype. Similar observations have also been reported for human ES cells [30,31]. However, little progress has been made on the analyses of EPCAM expression and its function in the germline.

In the present study, EPCAM expression changed dynamically during SSC differentiation. We originally hypothesized that given its strong expression on GS cells, EPCAM would be a useful antigen for selection of a pure spermatogonial population from the testis in order to initiate GS cell culture without contamination by testicular somatic cells. However, EPCAM-selected cells had limited clonogenic activity in vitro, and showed strong KIT expression, suggesting that they were more enriched for progenitor spermatogonia compared with CD9-selected cells. Double immunostaining and transplantation of fractionated CD9-selected cells revealed that $CD9^{-}EPCAM^{low/-}$ cells showed little KIT expression, and had significantly increased SSC activity. These results support the suggestion that EPCAM is gradually upregulated in SSCs as they differentiate into progenitor spermatogonia in vivo.

EPCAM upregulation during SSC differentiation was unexpected, because EPCAM has been considered a useful marker for SSCs, including those in rat and humans [11,32], and is strongly expressed on mouse GS cells. In fact, EPCAM was reported to be the best marker for rat SSCs [11]. Another study in rats also demonstrated clonogenic activity of EPCAM-expressing gonocytes [33]. Although these previous results strongly suggested that EPCAM expression in SSCs is conserved across different species, our results in mouse cells showed that EPCAM is regulated in a more sophisticated manner, being most strongly expressed in progenitor spermatogonia. The mechanism of SSC commitment has been a major topic of recent SSC research, but the lack of appropriate cell surface makers has prevented detailed analyses. EPCAM appears to be a useful cell surface marker for fractionating the spermatogonial compartment in studies of SSC self-renewal and differentiation. Our results also underscore the importance of functional transplantation studies based on the quantitative assessment of cell surface marker expression levels. It will be interesting to learn whether similar EPCAM expression patterns are conserved during spermatogenesis in other animal species.

The regulation and function of EPCAM were analyzed using GS cells, a pure proliferating spermatogonial cell population. EPCAM was upregulated by GDNF, suggesting that strong EPCAM expression in GS cell cultures is attributable in part to continuous exposure to GDNF, which is necessary for the propagation of SSCs in vitro. In contrast, FGF2 showed no apparent effect on EPCAM expression, although it is also an indispensable cytokine for GS cell culture. In ES cells, EPCAM

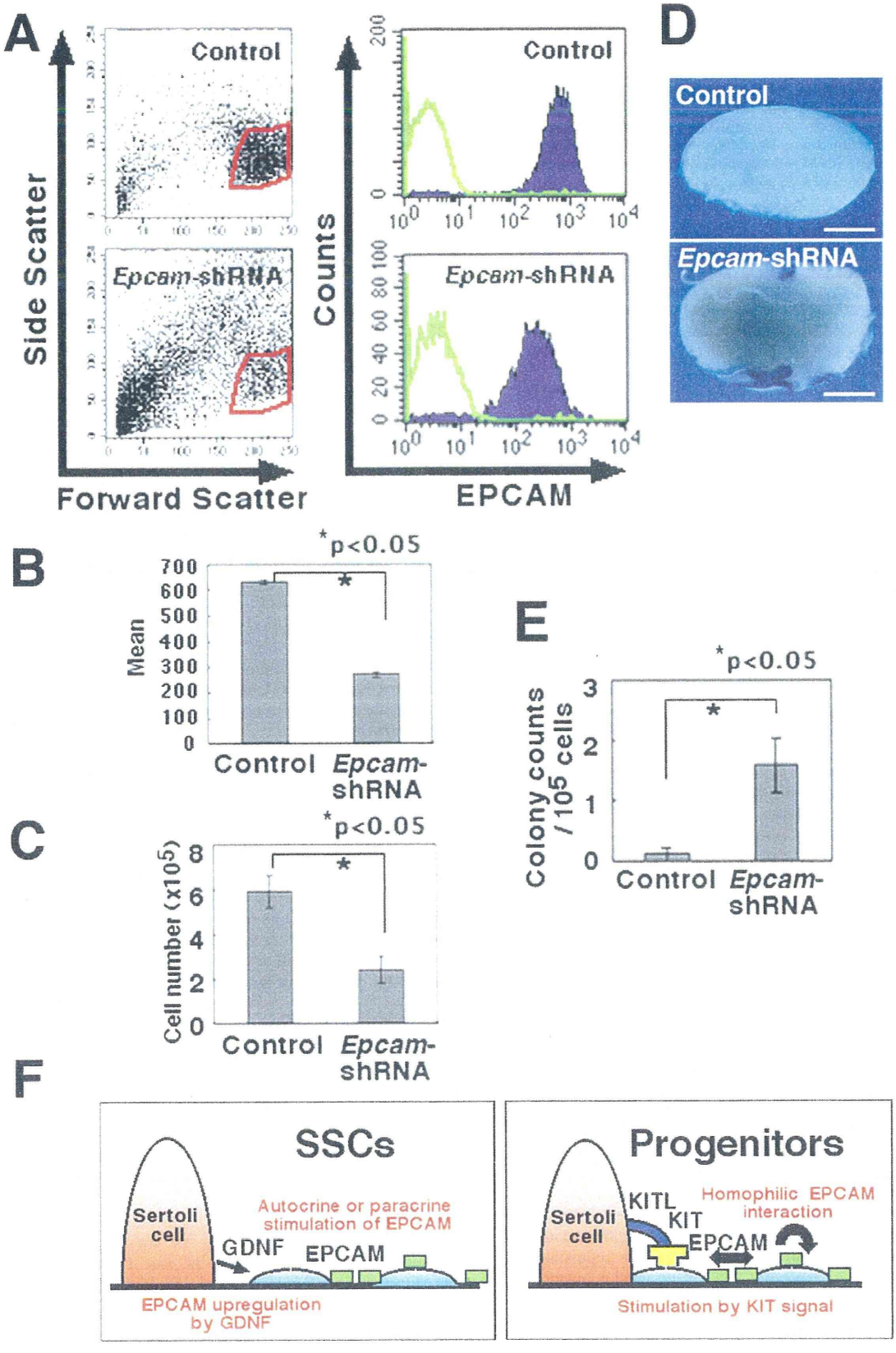
A
Control
Epcam-shRNA
Side Scatter
Forward Scatter
Counts
EPCAM
D
Control
Epcam-shRNA
B
*p<0.05
Mean
Control
Epcam-shRNA
C
*p<0.05
Cell number (x10^5)
Control
Epcam-shRNA
E
*p<0.05
Colony counts / 10^5 cells
Control
Epcam-shRNA
F
SSCs
Sertoli cell
GDNF
EPCAM
Autocrine or paracrine stimulation of EPCAM
EPCAM upregulation by GDNF
Progenitors
Sertoli cell
KITL
KIT
EPCAM
Homophilic EPCAM interaction
Stimulation by KIT signal

Figure 5. *Epcam* KD in ROSA GS cells by shRNA. (A) Flow cytometric profile of ROSA GS cells 2 days after transduction with *Epcam* KD vector. Green lines indicate controls. (B) Expression of EPCAM represented by the mean fluorescence intensity. Data are expressed as mean fluorescence intensity minus background autofluorescence of cells stained with the control secondary antibody. (C) Reduced recovery of ROSA GS cells after transduction with shRNA against *Epcam*. GS cells (8×10^5) on MEFs were infected with the lentivirus and recovered 2 days later. Results of three experiments are shown. (D) Macroscopic appearance of the recipient testes transplanted with *Epcam* KD GS cells. The same number of cells was transplanted at the same time. Blue tubules indicate germ cell colonies developed from donor SSCs. (E) Assessment of SSC activity by germ cell transplantation. ROSA GS cells were transplanted into the seminiferous tubules of W mice 3 days after transduction with shRNA against *Epcam*. (F) A model for EPCAM function during SSC differentiation. GDNF upregulates EPCAM expression on SSCs/progenitors. Proliferation/survival of progenitors may be stimulated by EPCAM expression on neighboring cells as well as by KITL on Sertoli cells. Stain: X-Gal (D). Bar = 1 mm (D).
doi:10.1371/journal.pone.0023663.g005

expression is upregulated by LIF. Thus, our results indicate that the regulation of EPCAM expression differs between ES cells and germline cells. In GS cell culture, LIF is useful for initiating cultures from gonocytes, but is dispensable for establishment of GS cells from spermatogonia. We also have not been able to observe a positive effect of LIF on GS cell maintenance [34]. It may be that EPCAM expression changes in accordance with the cytokine milieu of the testicular micronevironment.

Although we did not find a significant effect of EpICD overexpression, the downregulation of EpICD by *Epcam* KD treatment significantly suppressed the GS cell recovery. This suggested that EPCAM is involved in proliferation or survival of spermatogonia. Interestingly, transplantation of *Epcam* KD cells resulted in a relative enrichment of SSCs. Given the in vivo expression pattern, these results suggest that EPCAM plays an important functional role in progenitor cell compartment. At present, very little is known about how progenitor spermatogonia increase their numbers in vivo. KIT is one factor involved in spermatogonial proliferation/survival [20]. Although its inhibition by neutralizing antibody kills a large number of proliferating spermatogonia [20], the inhibition of KIT signaling did not interfere with GS cell proliferation [35]. Similarly, the addition of KITL (Steel factor) did not enhance GS cell proliferation. Therefore, KIT does not appear to be vital in GS cell proliferation. The present results suggest that EPCAM may be a good candidate for progenitor cell proliferation. Cell-to-cell contact has been identified as an initial trigger for EPCAM activation [27]; therefore, we speculate that upregulated EPCAM on the cell surface may stimulate the proliferation of neighboring spermatogonia by shedding extracellular domain of EPCAM, thereby creating a positive feedback loop on proliferation signal in an autocrine or paracrine fashion [14]. This provides an additional stimulus to KIT, the ligand of which is expressed on Sertoli cells [20]. The availability of two different stimuli in parallel may perhaps contribute to the marked expansion of spermatogonia progenitors during differentiation (Fig. 5F).

The fractionation of CD9-selected cells based on EPCAM expression significantly improved the SSC purification efficiency. Subfractionation of the CD9-selected cells resulted in more efficient selection and achieved 48.7-fold enrichment. Assuming that 10% of SSCs can colonize seminiferous tubules [5], the frequency of SSCs in the suspension was 1 in 115 cells. Hence, this method appears to be more efficient than the in vivo enrichment method using cryptorchid testes, in which 1 in 161 cells were SSCs [36]. The high SSC activity in $CD9^{-}EPCAM^{low/-}$ cell population was in agreement with stronger expression of several spermatogonia molecules implicated in SSC self-renewal, including *Nanos3*, *Bcl6b*, and *Etv5* [8,22]. However, the expression level of *Nanos2*, which is thought to be expressed in the most undifferentiated spermatogonia [21], was relatively weak in the same population, possibly be due to its low expression level or the small population size.

Previous attempts to enrich SSCs were based on cryptorchid mouse models with only undifferentiated spermatogonia. Although SSCs have now been purified to 1 in 15 to 30 cells by sorting of cells from the cyptorchid testes, the preparation of cryptorchid testes requires at least 2 months to remove differentiating germ cells [36], and the technique may not be applicable to many animal species due to differences in anatomical structures. We also cannot exclude the possibility that SSCs in cryptorchid testes have different biological characteristics from those in wild-type controls. For example, a recent study showed that KIT-expressing progenitor spermatogonia from wild-type testes can generate SSCs [37]. This was in contrast to our previous study that showed the absence of KIT on SSCs collected from cryptorchid testes [6]. In the present study, SSC activity was enriched in the $CD9^{-}EPCAM^{low/-}$ cell population, which consisted predominantly of $KIT^{low/-}$ cells. However, this population also contained some KIT^{-} cells. Although we recently reported that both KIT^{-} and KIT^{-} cell populations in GS cell culture showed comparable levels of SSC activity [35], only KIT^{-} cells showed SSC activity after transplantation, which suggested that KIT expression on SSCs may change according to their environment. Therefore, it is important to establish methods to purify SSCs from wild-type testes, and introduction of KIT as an additional marker may not only reconcile these conflicting observations but also improve the purification efficiency.

Ideally, the identification of SSC-specific antigens will greatly advance our understanding of SSC biology, as the lack of such markers has limited our knowledge regarding the regulation of SSC self-renewal and differentiation. Although the morphological description of spermatogonia has been well established, little progress has been made in the functional analysis of this compartment. Our results suggest that EPCAM is a useful marker for characterizing the spermatogonial compartment, and our analyses suggest that it plays an important role in spermatogonial progenitor proliferation or survival. The future analysis of this molecule will not only contribute to an improved SSC purification strategy but also increase our knowledge of SSC commitment.

Supporting Information

Table S1 PCR primers.
(DOC)

Acknowledgments

We thank Ms. Y. Ogata for technical assistance, and Dr. O. Gires for the generous gift of EpICD cDNA.

Author Contributions

Conceived and designed the experiments: TS MKS. Performed the experiments: TS MKS KI ST. Analyzed the data: TS MKS KI ST. Contributed reagents/materials/analysis tools: TS. Wrote the paper: TS MKS.